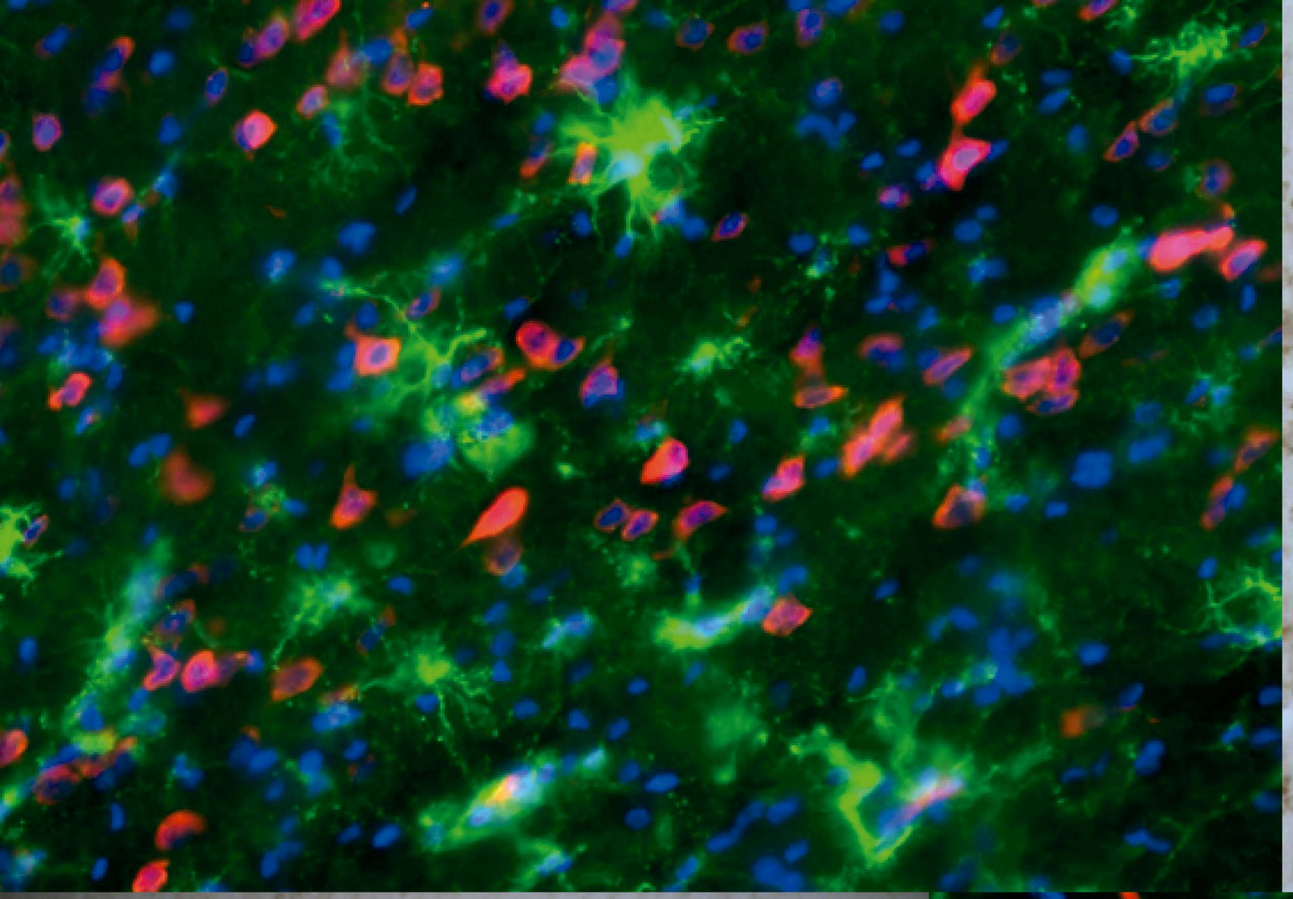
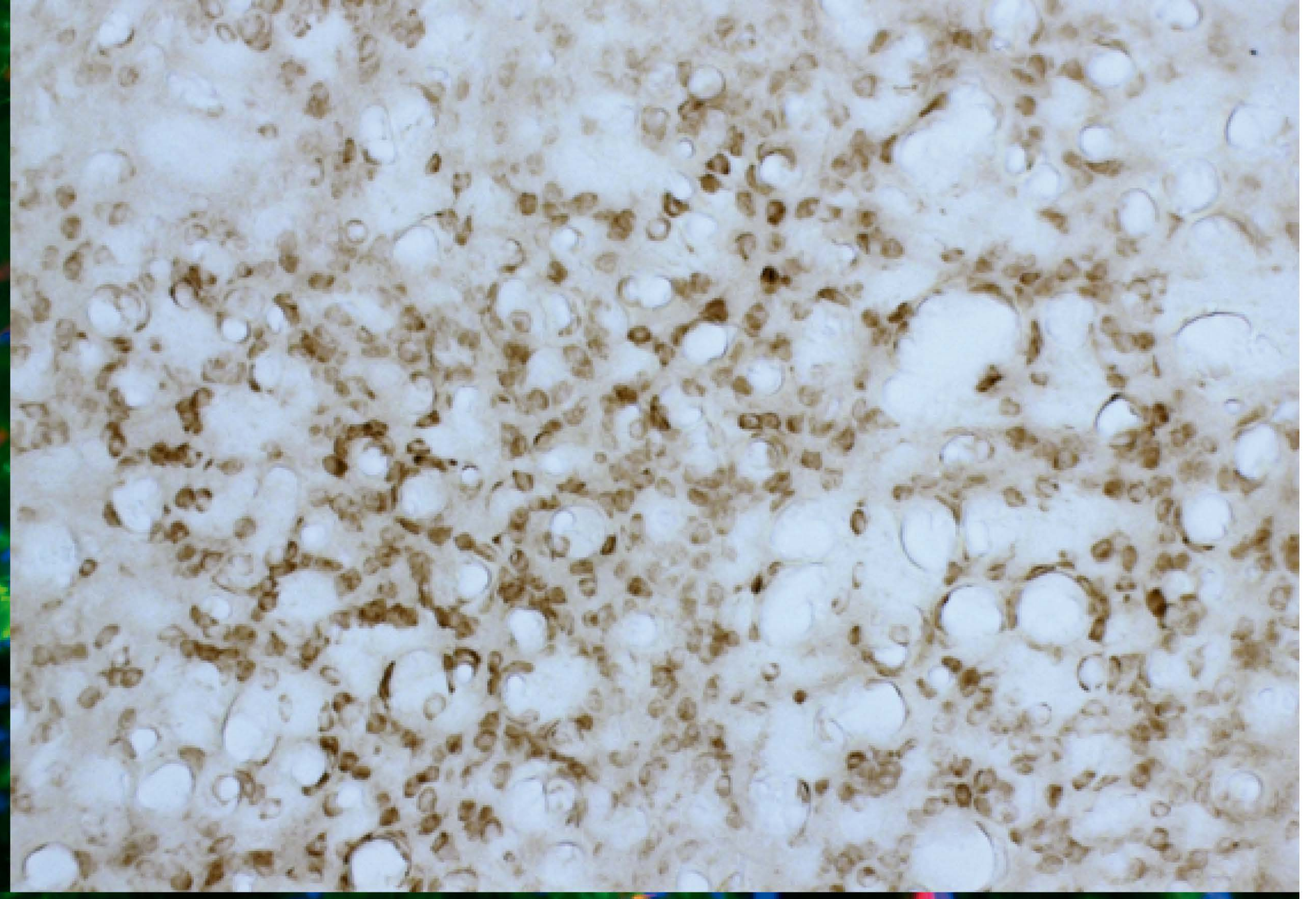
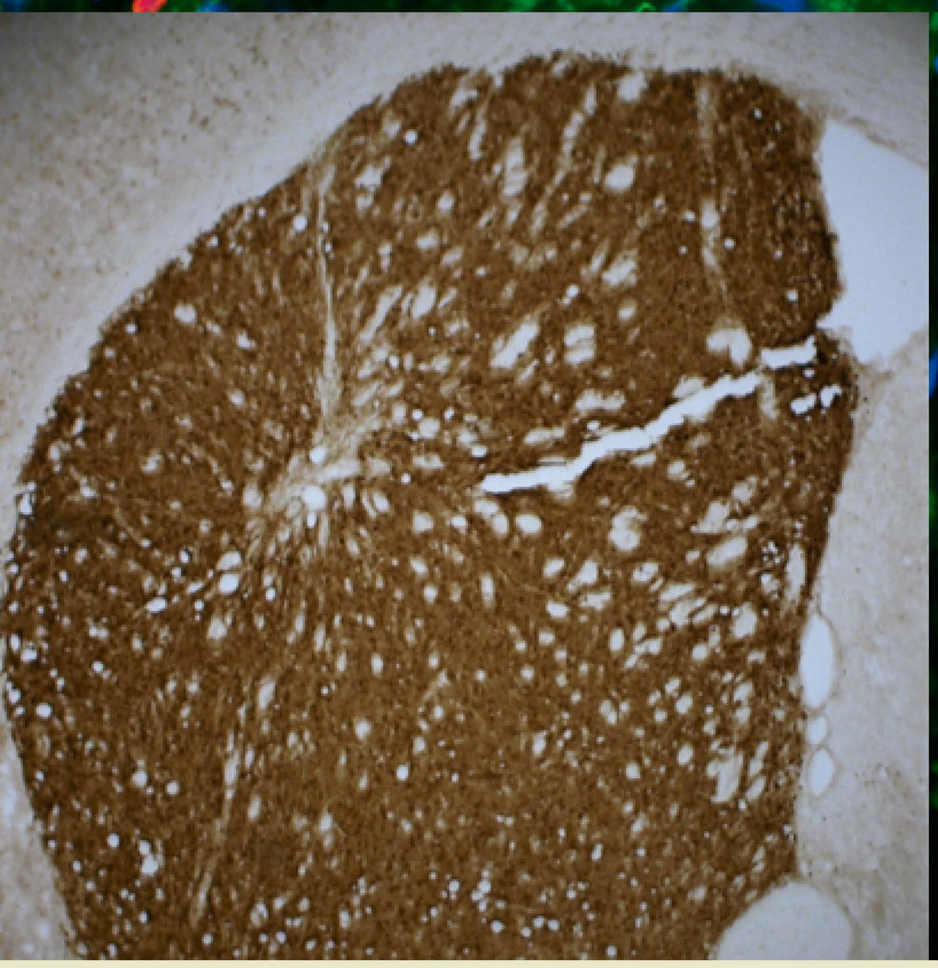
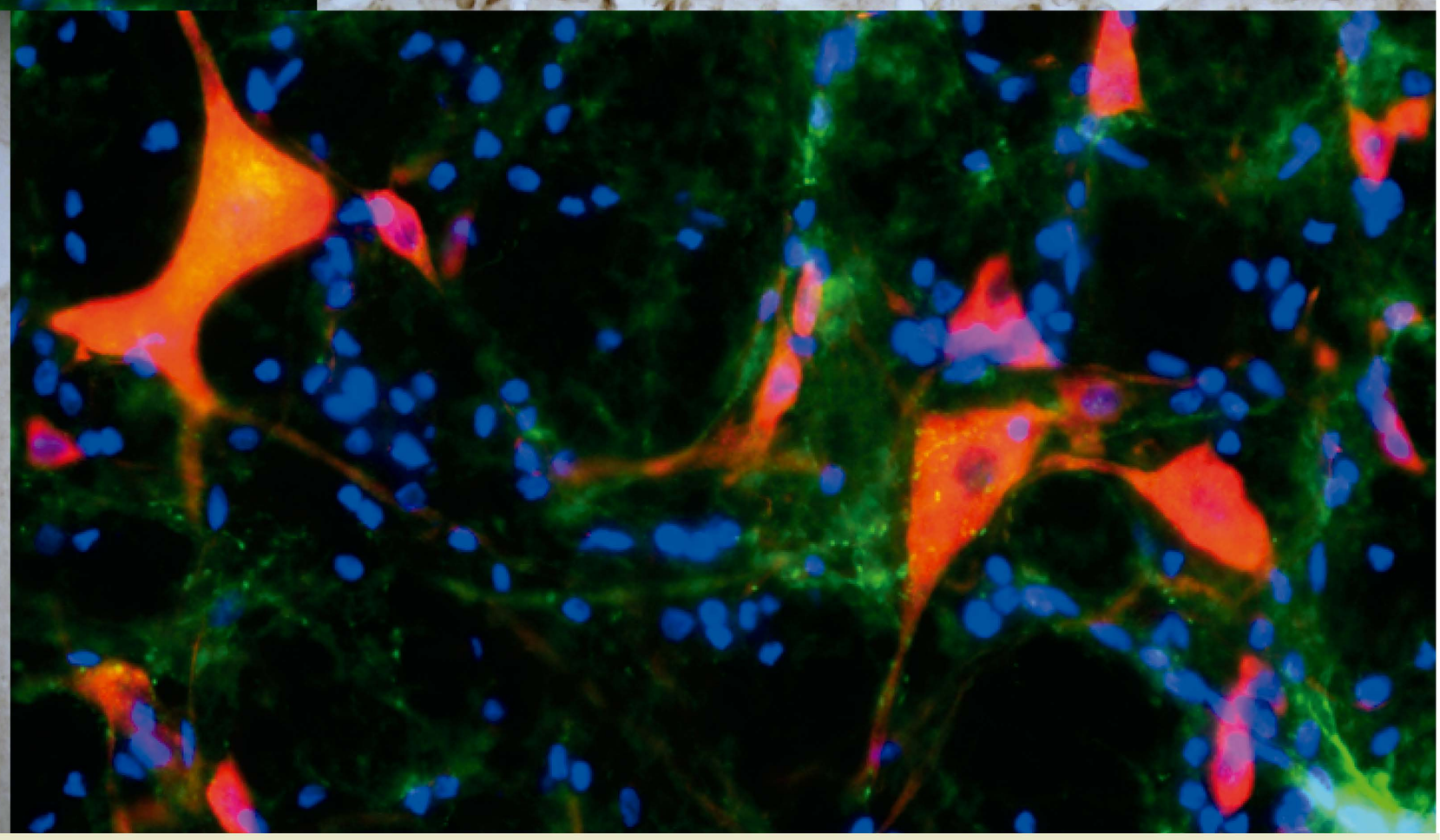

João Miguel da Conceição Alves do Cruzeiro

Development of a striatal lentiviral mouse model of Spinocerebellar Ataxia type 2

Dissertação de Mestrado em Biologia Celular e Molecular com especialização em neurobiologia,
sob a orientação do Doutor Clévio David Rodrigues Nóbrega e do Professor Doutor Carlos Jorge Alves Miranda Bandeira Duarte,
apresentada ao Departamento de Ciências da Vida da Faculdade de Ciências e Tecnologia da Universidade de Coimbra.

Julho 2016

· U C ·

UNIVERSIDADE DE COIMBRA

UNIVERSIDADE DE COIMBRA

João Miguel da Conceição Alves do Cruzeiro

Development of a striatal lentiviral mouse model of Spinocerebellar ataxia type 2

Dissertação apresentada à Universidade de Coimbra para cumprimento dos requisitos necessários à obtenção do grau de Mestre em Biologia Celular e Molecular com especialização em Neurobiologia, realizada sob a orientação científica do Doutor Clévio David Rodrigues Nóbrega (Centro de Neurociências e Biologia Celular, Universidade de Coimbra) e sob orientação interna do Professor Doutor Carlos Jorge Alves Miranda Bandeira Duarte (Departamento de Ciência da Vida, Universidade de Coimbra).

Julho, 2016

Front cover composed of 4 separated images.

Upper left image: immunohistochemistry with fluorescent staining for ataxin-2 (mouse, 1:750, BD biosciences, red), GFAP (rabbit, 1:1000, DAKO, green) and DAPI (blue) in the *striatum* of mice.
Upper right image: light immunohistochemistry with staining for ataxin-2 (rabbit, 1:500, Millipore), in the *striatum* of WT mice injected with ATXN2MUT.
Lower left image: light immunohistochemistry with staining for DARPP32 (rabbit, 1:1000, Millipore) in the *striatum* of WT mice injected with ATXN2MUT.
Lower right image: immunohistochemistry with fluorescent staining for ataxin-2 (mouse, 1:750, BD biosciences, red), GFAP (rabbit, 1:1000, DAKO, green) and DAPI (blue) in the *cerebellum* of mice.

The present work was performed in the Viral Vectors and Gene Therapy group of the Center for Neuroscience and Cell Biology (University of Coimbra, Portugal), headed by Professor Luis Pereira de Almeida, and under supervision of Doctor Clévio Nóbrega and Doctor Liliana Mendonça.

Para os meus queridos pais
e para o meu irmão Luis

Acknowledgments/Agradecimentos

Em primeiro lugar gostaria de agradecer ao Doutor Clévio Nóbrega, por ter acreditado em mim quando mais precisava e por me ter convidado para este projecto. Ao longo deste ano, a sua orientação, exigência, disponibilidade e compreensão fizeram com que me mantivesse constantemente motivado e que a pesada carga horária, característica de uma tese de mestrado, se "diluísse" num agradável e motivador ambiente de trabalho. Gostaria também de realçar o profissionalismo e a maneira hábil com que soube orientar os seus três alunos de mestrado, permitindo desta forma que se criasse um grupo unido e com laços fortes de entreajuda entre os três orientandos. No global, considero de facto a sua orientação irrepreensível, e espero que um dia possa vir a trabalhar com ele de novo.

Gostaria também de agradecer ao Professor Doutor Luís Almeida por me ter recebido no seu laboratório de braços abertos, estando sempre disponível para ajudar com qualquer tema, relacionado ou não com a tese. A sua agenda, por muito que esteja preenchida pela responsabilidade de orientar e manter unido um grupo com mais de 20 pessoas, nunca foi impedimento para vir dirigir um sorriso e uma palavra de encorajamento aos seus alunos antes de se ir embora. Esta atitude ficou-me marcada ao longo deste ano porque denota o respeito que tem por todos os elementos do seu grupo de investigação.

Um agradecimento também à Professora Doutora Cláudia Cavadas por ter tido as portas do seu laboratório sempre abertas para mim, apesar de não pertencer directamente ao seu grupo, e por nunca se escusar de me dirigir uma palavra de ânimo sempre que me encontra.

Gostaria de deixar um agradecimento especial à Liliana, por me ter ensinado quase tudo o que sei de trabalho de bancada e nunca me ter deixado desanimar com os maus resultados. Fiquei impressionado com o profissionalismo e exigência com que trata os seus alunos, mas que nunca é maior do que aquilo que exige de si própria. A sua capacidade de trabalho, compreensão e irredutível optimismo foram contagiantes para mim, bem como a enorme disponibilidade com que me recebia, sempre que a ia "melgar". Ao longo deste ano recebi inúmeros ensinamentos seus, que nem sempre foram científicos mas também de conduta, atitude, resiliência, entre outros.

Quero também agradecer à Filipa pela ajuda preciosa com os testes de comportamento, bem como pela sua amizade e espírito de entreajuda. Sem ela, não poderia com toda a certeza ter apresentado um dos capítulos da tese.

À Sara Silva por me ter ajudado nos primeiros "passos" que dei no mundo da ciência experimental, pela disponibilidade incondicional com que sempre me recebeu e pela ajuda preciosa com os Western-blots.

A ciência se fosse um desporto, seria sem dúvida um desporto colectivo. As melhores equipas serão sempre mais eficazes do que os elementos individuais, e por isso me sinto profundamente grato por ter integrado este grupo de pessoas. Sem elas, este trabalho não teria sido possível.

Contudo, houve todo um outro conjunto de pessoas que, apesar de não terem contribuído directamente, facilitaram sem dúvida aquilo que foi um ano difícil mas enriquecedor. Entre essas pessoas, gostava de realçar todos os elementos dos grupos LA&CC pela ajuda e pela simpatia prestadas, em particular aqueles que me foram mais próximos como a Dina, a Sara, a Patrícia, a Ana Cristina, o Vítor e a Janete. A todos eles agradeço a ajuda científica mas também o apoio, os momentos de boa-disposição bem como os convites para jantar e "lavar" a cabeça da tese, por um momento que fosse. Gostava também de agradecer a todos os meus colegas e amigos do Mestrado em Biologia Celular e Molecular, em especial àqueles que fizeram a sua tese no CNC e que partilharam comigo as dificuldades, os deadlines, os maus resultados, os horários loucos e a escrita da tese. Devo dizer que foi de facto uma honra ter pertencido a esta grande geração de 2014-2016 de BCM. Quero também agradecer ao professor Carlos Duarte pela sua dedicação a este mestrado e a todos os seus alunos e por ter sido, muito provavelmente, o melhor professor que alguma vez tive.

Por fim também quero agradecer a toda a minha família e aos meus amigos de sempre (que são a família que escolhemos para nós próprios) pelos almoços e jantares, conversas, jogos de futebol, jogos de basket, saídas, viagens e todas essas coisas que fazem a vida valer a pena. Deixo um agradecimento especial à minha avó Francelina (que faz este ano 90 anos) por me ter ensinado que o optimismo e a autoconfiança afinal também me correm nas veias, e à minha avó Floripes por me ensinar a nunca deixar de lutar, independentemente das circunstâncias. Também quero agradecer aos meus pais e ao meu irmão Luis por aturarem as minhas loucuras, por terem suportado o meu mau humor nestes últimos meses e pelo apoio incondicional prestados. Eles têm o papel mais difícil de todos, e esta tese é dedicada a eles.

Finalmente, quero agradecer à Katty por me ter ensinado tantas coisas da vida, que nada têm a ver com ciência, mas que são tão mais importantes. O destino foi caprichoso

connosco, mas o que quer que seja que o futuro nos reserva, terás sempre um lugar especial no meu coração. Muito obrigado!

Index

Abbreviations

A2D – Ataxin-2 domain protein

ALS - Amyotrophic lateral sclerosis

BAC - Bacterial Artificial Chromosomes

BBB - Blood-brain barrier

BSA - Bovine Serum Albumin

cDNA - Complementary DNA

CD11B – Cluster of differentiation molecule 11B

CNS – Central nervous system

Ct - threshold cycle

DARPP-32 – Dopamine- and cAMP-regulated neuronal phosphoprotein 32

DAT - Dopamine active transporter

DRPLA - Dentatorubral Pallidoluysian Atrophy

EIF4E – Eukaryotic translation initiation factor 4E

EIF4G – Eukaryotic translation initiation factor 4G

EtOH - ethanol

GFAP – Glial Fibrillary Acid protein

GADPH – Glyceraldehyde 3-phosphate dehydrogenase

GM130 – Golgi matrix protein 130

HD - Huntington's disease

HEK - Human embryonic kidney

HIV-1 – Human immunodeficiency virus 1

HPRT – Hypoxanthine-guanine phosphoribosyl-transferase

ip - intraperitoneal

Iba-1 - Ionized calcium-Binding Adapter molecule 1

KO – Knockout

Kb – Kilo base

KDa – Kilo Dalton

KI - Knock-in

Lsm - Like Sm domain

LsmAD - Lsm-associated domain

MJD - Machado-Joseph disease

MRI - Magnetic resonance imaging

NGS - Normal Goat Serum

P62/SQSTM – Sequestosome 1

PABP - Poly(A)-binding protein

PAM2 – PABPC interacting motif-2

PBS - phosphate-buffered saline

PC - Purkinje cell

Pcp2 - Purkinje cell protein 2

PD – Parkinson's disease

PGK - Phosphoglycerate Kinase 1

PolyQ - Polyglutamine

PSD-95 – post-synaptic density protein-95

qRT-PCR – quantitative Real-time polymerase chain reaction

rER - rough endoplasmic reticulum

RIPA - Radio-Immunoprecipitation Assay

RPL14 – Ribosomal protein L14

SBMA - Spinal Bulbar Muscular Atrophy

SCA - Spinocerebellar ataxia

SCA2 - Spinocerebellar ataxia type 2

SIN - self-inactivating

SK2/3 - Small-conductance, Ca^{2+}-activated K^{+} channels Type 2/3

PVDF - polyvinylidene fluoride

SYP – Synaptophysin

TBS-T - Tris buffered saline

UTR – Untranslated Region

VGLUT - Vesicular glutamate transporter

Lists of Tables and Figures

List of Tables

List of Figures

List of Supplementary Figures

Abstract

Spinocerebellar ataxia type 2 (SCA2) is an autosomal dominant ataxia caused by an expansion of 'CAG' repeats in the exon 1 of the gene ATXN2, conferring a gain of toxic function that triggers the appearance of the disease phenotype. The disease is characterized by several symptoms including progressive gait ataxia and dysarthria, slow saccadic eye movements, sleep disturbances, cognitive impairments and psychological dysfunctions such as insomnia and depression, among others. The available treatments rely on palliative care alone, which mitigate some of the major symptoms but ultimately fails to block the disease progression. This current lack of effective therapies highlight the need to create new platforms, allowing the study of the disease molecular basis and the development of new therapeutic strategies. For many years, this depended upon the analysis of postmortem tissues from deceased patients, which can provide data with great biological significance but are limited to the terminal stages of this disease. However, the identification of the causative mutation related to SCA2 and the development of state-of-the-art molecular technologies paved the way for the creation of some models in yeast, *C. elegans*, *D. melanogaster* and mice. These models have provided the researchers with greater insight into the molecular pathways of the disorder to reinforce the human patient's data. Furthermore, a set of 4 transgenic and 1 knock-in mouse successfully recreated many of the SCA2 major symptoms, including gait ataxia, motor incoordination and neuropathological features such as ataxin-2 inclusions and cerebellar degeneration. This set of characteristics make these mice invaluable to deepen our understanding of the human disease and also reliable platforms to test for new therapeutic alternatives.

Notwithstanding this, the available models have focused mainly on the cerebellar dysfunctions that characterize SCA2, while other brain regions and their contributions to the pathophysiology of this disease remain generally unexplored. Indeed, the anomalies in the *cerebellum* cannot explain all of the symptoms displayed by the human patients, suggesting that other brain areas might be affected as well. One of these areas is the *striatum*, which has been reported to display mutant ataxin-2 inclusions and neurodegeneration, that might be responsible for the cognitive impairments and the parkinsonism often observed in patients.

In this work, we have used lentiviral vectors to overexpress a full-length mutated version of ataxin-2 in the *striatum* of C57BL/6 mice, successfully inducing a neuronal dysfunction

phenotype. However, no ubiquitinated inclusions were detected nor a neuroinflammatory response was observable at 8 weeks of age. Interestingly, this time point was enough to detect a clear synaptic dysfunction in the *striatum*, which could be the cause for the hyperactive exploratory behavior displayed by these mice. Furthermore, the unilateral injection of ATXN2MUT in the *striatum* induced a mild *ipsilateral* turning behavior that suggests impairment in the dopaminergic transmission. In conclusion, we present an alternative modeling strategy for SCA2 that might disclose the contribution of the *striatum* to disease progression and study particular characteristics of this disorder that were not possible with the existing models.

Keywords: Spinocerebellar ataxia type 2 (SCA2), ataxin-2, *striatum*, lentivirus, animal models of disease

Resumo

A ataxia espinocerebelosa do tipo 2 (SCA2) é uma doença genética autossómica dominante que tem como causa uma expansão do trinucleótido 'CAG' no exão 1 do gene ATXN2. Este número anormal de repetições confere propriedades tóxicas à proteína ataxina-2, resultando em morte e disfunção neuronal e induzindo assim o desenrolar da patologia. Esta doença é caracterizada por uma série de sintomas de carácter progressivo, como por exmplo: ataxia locomotora, disartria, distúrbio dos movimentos oculares sacádicos, perturbações do sono, disfunções cognitivas e perturbações psiquiátricas como depressão, insónias, entre outros. Até à data, não existe nenhum tratamento que modifique a progressão da doença, sendo que as únicas opções terapêuticas consistem em medidas de cuidados paliativos e de melhoria da qualidade de vida. Esta situação apela à criação de novas plataformas de estudo da SCA2 que permitam estudar em maior detalhe o desenvolvimento da doença, bem como testar novas alternativas terapêuticas. Durante vários anos, estes estudos estavam limitados à análise de tecidos *post-mortem* de doentes, que naturalmente estavam limitados ao estádio terminal da doença. Este facto impossibilitava o estudo dos primeiros mecanismos moleculares que levam ao seu desenvolvimento. No entanto, esta situação foi revertida com a descoberta da mutação causadora de SCA2, e a consequente criação de vários modelos celulares e animais em leveduras (*Saccharomyces cerevisiae*), nemátodes (*Caenorhabditis elegans*), mosca-da-fruta (*Drosophila melanogaster*) e ratinho (*Mus musculus*). Estes estudos permitiram aprofundar os mecanismos moleculares por detrás da doença e também as funções celulares da proteína ataxina-2, reforçando assim os dados provenientes de tecido humano. Por fim, o desenvolvimento de vários modelos transgénicos e de knock-in em ratinhos possibilitou recriar vários sintomas de SCA2 nos animais, incluindo descoordenação motora, degenerescência do cerebelo e a formação de agregados de ataxina-2. Estes animais constituem assim um recurso valioso para aprofundar o nosso conhecimento desta patologia bem como para testar o efeito de novos fármacos e estratégias terapêuticas.

No entanto, os modelos descritos até ao momento focam-se quase exclusivamente numa única zona do cérebro – o cerebelo – relegando para segundo plano outras regiões que também estão envolvidas em SCA2. Uma destas zonas é o estriado, no qual já foi descrito em doentes a presença de inclusões ubiquitinadas bem como neurodegenerescência. O facto de muitos doentes sofrerem de Parkinsonismo, chegando até a responder positivamente ao

tratamento com Levodopa, parece reforçar a tese de que o estriado contribui para o desenvolvimento da patologia, apesar deste tópico não estar de todo esclarecido.

No decorrer deste projeto, usámos lentivirus recombinantes para induzir a expressão de ataxina-2 mutante no estriado de ratinhos WT, e gerámos com sucesso um fenótipo de disfunção neuronal nesta região cerebral. Apesar de não termos observado a presença de inclusões ubiquitinadas nem de uma resposta neuroinflamatória clara, descrevemos uma série de alterações nos níveis de proteína e RNA de vários constituintes sináticos, bem como alterações comportamentais exibidas por estes animais. Por fim, também observámos que os animais injetados unilateralmente com ataxina-2 mutante possuem um comportamento rotativo tendencioso, indicando uma possível disfunção na transmissão dopaminérgica do estriado. Em resumo, nesta dissertação apresentamos uma estratégia alternativa para modelar a ataxia espinocerebelosa do tipo 2 em ratinho, que contribuiu para aprofundar o papel do estriado no desenvolvimento da patologia. Também acreditamos que no futuro será um modelo valioso para estudar determinadas características desta doença que não seriam possíveis com outros modelos existentes.

Palavras-chave: Ataxia espinocerebelosa do tipo 2 (SCA2), ataxina-2, estriado, lentivirus, modelos animais de doença

Chapter I - Introduction

Tri-nucleotide expansion diseases

The beginning of the 1990's was marked by the identification of a particular set of neurological and muscular diseases that are caused by an expansion of unstable trinucleotide repeats [1, 2]. These triplet repeats are highly polymorphic and unstable in the human population, making them susceptible for expansion during mitosis and/or meiosis [3]. Based on this fact, scientists soon related the size of those expansions with the phenotypic variability found in the disorders: bigger tri-nucleotide expansions results in an earlier disease onset and severer symptoms. Since then, a total of 16 neurological disorders have been causally correlated to mutations of this kind, including the Fragile-X mental retardation syndrome, myotonic dystrophy and Huntington's disease (HD) [4, 5]. This last one is included in a particular group called the polyglutamine (PolyQ) diseases that are caused by an expansion of the 'CAG' triplet, resulting in an expanded polyglutamine tract in the affected protein (see figure 1). Together with HD, other traits such as Machado-Joseph disease and 5 other spinocerebellar ataxias (SCA-1, 2, 6, 7, 17) as well as Dentatorubral Pallidoluysian Atrophy (DRPLA) and Spinal Bulbar Muscular Atrophy X-linked type (SBMA) were determined to constitute the PolyQ disorders known to date [6]. With the exception of SBMA, PolyQ's are autosomal dominant and inherited in a mendelian manner with a frequency of 1-10 affected individuals per each 100'000 people [7]. This work will focus in spinocerebellar ataxia diseases with a particular emphasis in SCA2.

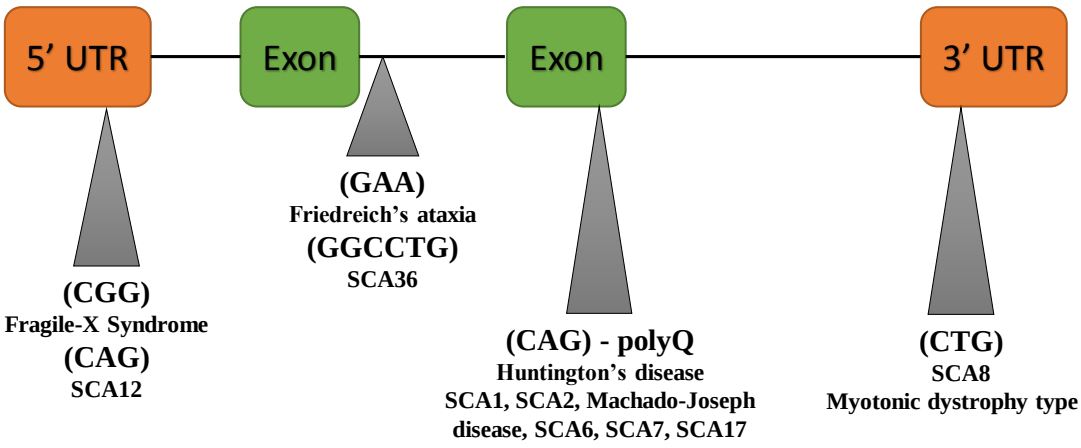

Figure 1. Trinucleotide expansion diseases. Schematic representation of the tri-nucleotide expansion diseases, including the location (intronic, exonic, UTRs) and the expanded tri-nucleotides associated with the disorders.

Spinocerebellar ataxias

SCAs are a group of autosomal dominant neurodegenerative diseases characterized by a wide variety of cerebellar as well as extracerebellar symptoms that usually manifest during adulthood. This body of disorders display clinical, genetic, and neuropathological heterogeneity, depending on the affected gene and on the size of the expansion [8]. However, they all share the common end point of cerebellar, and particularly Purkinje cell (PC) degeneration, resulting in a panel of symptoms that include gait ataxia, cerebellar dysarthria, dysmetria, adiadochokinesia, and postural tremor. These often come together with extracerebellar manifestations such as cognitive dysfunction, pyramidal and extrapyramidal signs, visual impairment, peripheral neuropathy and psychiatric alterations, comprising the panel of the most common symptoms associated with SCAs [9]. From this point forward, and for the purposes of this work, we will apply the general term - SCAs – to refer to the large subgroup of SCAs that belong to the PolyQ disorders, caused by an expansion of the 'CAG' triplet. Nevertheless, there are other varieties such as SCA10, SCA12 or SCA36 that are caused by conventional mutations in critical genes, or expansions in non-translated regions of the DNA like introns or the UTRs [10].

The prevalence of SCAs is considerably variable around the world, mostly due to particular phenomena of population's genetics in certain regions of the globe. One of these phenomena is the founder effect, which is directly related to colonization events. Indeed, if one of these founders has a very rare allele, the frequency of that allele in the colonized region will be highly increased, when compared to the population of origin. A very well-known example is the Azores Island "Flores" that has a considerably high prevalence (1:140) of Machado-Joseph disease, or SCA3, when compared to the global population (1-2 per 100'000 people) [11]. Another well-studied example is that of the Cuban province Holguín that has a SCA2 prevalence that reaches 141.66 affected individuals per 100'000 inhabitants (in the Baguanos municipality) due to the same peculiar event [12]. At the global scale, SCA3 is the most common ataxia in the world, with 21 % of cases, followed closely by SCA2 and SCA6 with 15 % [13].

Each of these diseases has a specific threshold – a given number of 'CAG' repeats – that delineates the border between the disease condition and the normal healthy condition (see table 1). This limit is variable between the different SCAs but any individual with a number of triplets above this threshold will develop the pathological phenotype [13]. In some of these diseases there is the so-called "pre-mutation" range, which corresponds to a number

of 'CAG' repeats that is higher than the average population but it still does not reach the threshold. Indeed, an individual with a triplet expansion that fits in this intermediate "pre-mutation" range does not develop the disorder, but has a high probability of having an affected progeny. This is due to the instability of this genetic region that can suffer an expansion in-between generations to reach the disease threshold [14]. Also, individuals affected with SCAs tend to have progeny with earlier disease onset and severer clinical manifestations, provoked by this increase in the number of 'CAG' repeats between generations [7]. This work will focus on a particular type of spinocerebellar ataxia - SCA2.

Table 1. Threshold values for the number of CAG repeats above which the SCA disease will develop. Table adapted from [6].

			Expanded CAG Repeats	
PolyQ Diseases	Locus	Protein	Normal	Pathological
SCA1	6p23	Ataxin-1	6–39	41–83
SCA2	12q24	Ataxin-2	14–32	34–77
SCA6	19p13	CACNA1A	4–18	21–30
SCA7	3p21–p12	Ataxin-7	7–18	38–200
SCA17	6q27	TBP	25–43	45–63
MJD/SCA3	14q24–q31	Ataxin-3	12–40	62–86

Spinocerebellar ataxia type 2

SCA2 was first known as Wadia–Swami type ataxia owed to the two Indian researchers that first reported this disorder [15, 16]. Later on, it became known as SCA2, after the identification of ATXN2 as the affected gene by three different groups [17–19]. The study of this disease assumes a central relevance in Hispano-American and Indian populations, since it has been demonstrated to be the most prevalent form of ataxia in Mexico, Holguín (Cuba) and eastern India [16, 20, 21]. However, the existence of large SCA2 families has also been reported in the UK [22, 23] and Spain [24, 25], where it is probably the most common SCA, and many other countries such as Australia, Germany, Italy, and Brazil. Worldwide, it is considered the second most common form of autosomal dominant cerebellar ataxia, together with SCA6, with 15% of total cases [13, 26].

Before the identification of the ATXN2 mutation, the diagnosis of this disease was based on observations of its major symptoms, which have little variation to the other SCAs. Thereby, SCA2 clinical manifestations include a slow and progressive gait ataxia and dysarthria accompanied by leg cramps, postural tremors, decreased muscle tone and decreased tendon reflexes [27]. These most often come together with visual impairments such as nystagmus, slow saccadic eye movements [28], sleep disturbances and, in some individuals, ophthalmoparesis [26, 27]. These clinical manifestations are usually triggered in the fourth decade of life in an affected individual and they tend to worsen in a progressive manner until the death of the patient, which typically occurs within 21 to 25 years after the onset of the disease phenotype [29]. In most cases, the physical symptoms come together with cognitive impairments like fronto-executive dysfunction, altered short-term memory, lack of attention [30], and psychological dysfunctions that end up in insomnia, depression, and suicidal impulses, as it was first uncovered by Reynaldo-Armiñán [cited in 15]. A more recent work by Raymond Lo and colleagues [31] included a follow-up of 64 SCA2 patients that revealed a strong prevalence of clinically relevant depression (22% of all patients) and suicidal ideation (almost 50%), similarly to other SCAs.

These clinical manifestations are usually the result of a neurodegenerative process that can be confirmed through the assessment of the neuropathology. In fact, the early post-mortem observations reported what would become one of the hallmarks of this disease: the anomalies in the *cerebellum* [32]. Indeed, this region of the brain that plays an important role in the motor coordination is consistently atrophied in post-mortem analysis of SCA2 patients, together with other regions such as the cerebral frontal lobes, brainstem, cranial nerves and spinal cord [32–34]. Interestingly, *in vivo* brain MRI of SCA2 patients has also revealed a significant atrophy of regions like the pontine base, the middle cerebellar peduncles and the cerebellar hemispheres, even when compared with SCA1 and SCA3 patients [28]. Also, recent studies have also found degeneration in the striatum, pallidum and the neocortex [32, 35].

At the cellular level, there is a severe reduction in the number of cerebellar PCs as well as its arborization [32, 36]. The cells of the granular layer also suffer neuronal loss, together with the brain stem and the *substantia nigra*, which might explain the parkinsonism observed in some patients [27]. This is a critical point, since SCA2 is the subtype of SCA that is most commonly associated with levodopa-responsive Parkinson's disease (PD) and atypical parkinsonism worldwide [37]. This overall degeneration in the brain of SCA2 patients goes far beyond the purely cerebellar alterations that its name might imply and it

ends up affecting the whole brain. This might somehow explain the variety of neurological symptoms associated with this disorder.

Although the presence of ataxin-2 aggregates remained quite controversial at first, several groups have presented compelling evidence for the existence of nuclear and cytoplasmic inclusions, similar to what happens in other polyQ diseases [33, 34, 38]. However, on an interesting note, these inclusions are often present in different regions of the brain except the *cerebellum*, which seems to remain clear of these aggregated structures.

Ataxin-2

The ATXN2 gene has 25 exons that encode for a 140 KDa protein, with 1312 amino acid residues (when it possesses 22 glutamines) and no sequence similarity to other polyQ proteins apart from the glutamine-rich domain [13]. Healthy individuals possess alleles of ATXN2 with 13-31 repeats of the 'CAG' triplets, located in exon 1, whereas a bigger number of repeats (that can go up to 200) results in the development of the disease [26]. Only one alternative spliced isoform has been conclusively identified so far [39], that encodes for a protein with 70 aa less than the canonical one. Interestingly, this alternative isoform seems to be the predominant form that exists in the *cerebellum*, which is the most affected brain region in SCA2. Subsequent studies are needed to deepen our understanding of this subject, namely an assessment of the toxicity of this isoform and its role in the pathophysiology of SCA2. The canonical isoform has two globular domains (see figure 2): the Lsm (Like Sm domain), associated with RNA binding functions such as decapping, splicing and degradation; and the LsmAD (Lsm-associated domain), that contains an exit signal for the rough endoplasmic reticulum (rER) [40, 41]. Other characteristic features of the ataxin-2 protein include the existence of proline-rich regions in the C- and N-terminals and the PAM2 motif in the exon 16. This last one is responsible for the interaction with the poly(A)-binding protein (PABP) [26]. The known structure of the protein together with several experiments made in simple models like yeast, *C. elegans* and *D. melanogaster* gave enough clues to infer on the ubiquitous functions of ataxin-2, such as: the embryonic development [42, 43]; the translation regulation and mRNA metabolism [44]; the regulation of circadian rhythms [45]; and modulating the formation of stress granules [46].

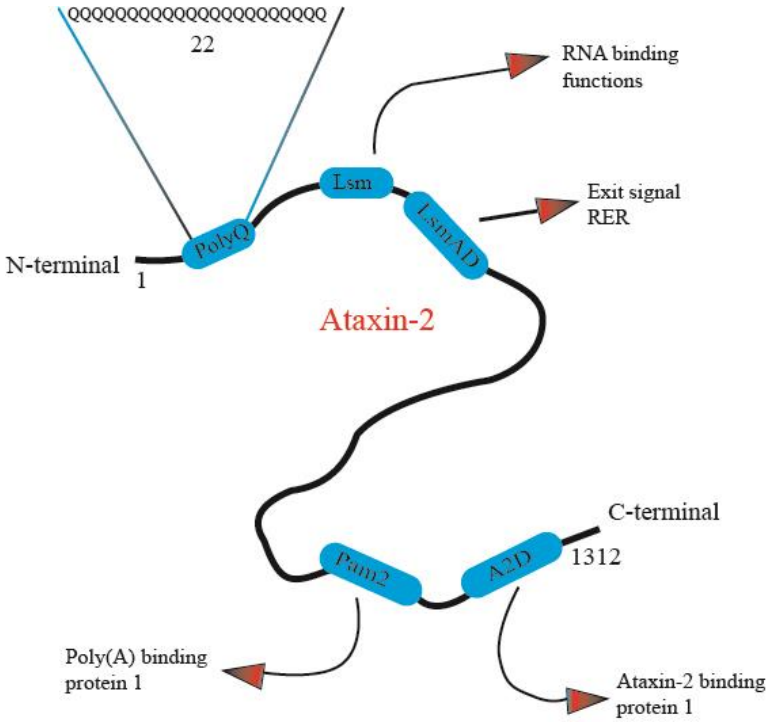

Figure 2. **Schematic representation of the protein ataxin-2, with 22 glutamines.** The protein has 1312 amino acids and a polyQ domain close to the N-terminal. The Lsm globular domain is conserved among RNA binding proteins, and is related with multiple functions such as decapping, splicing and degradation. The globular Lsm-Associated domain contains an exit signal for the rER. The Pam2 and the A2D domains are responsible for binding to the Poly(A) bindin protein 1 and to the Ataxin-2 binding protein 1, respectively.

Likewise, the creation and characterization of two murine KO models of ATXN2 have provided precious new insights into the functions and pathways of this protein [47–50] including a putative role in insulin resistance and obesity. All of these mechanisms related to ataxin-2 revealed a complex network of interactions and pathways regulated by this protein that somehow could explain the variety and the severity of SCA2 symptoms. This network, however, would become even more complex after several studies implicated ataxin-2 in the pathological process of amyotrophic lateral sclerosis (ALS) [51–53], SCA1 [54] and Machado-Joseph disease (MJD) [55–57]. These discoveries naturally increased the interest on this protein and its molecular pathways, since the deep understanding of its biology might help to devise strategies not only to SCA2, but also to other neurodegenerative conditions.

The existing therapies for SCA2 and other neurodegenerative diseases rely basically on palliative care and non-specific medication to alleviate the major symptoms, which is inefficient to halt the disease progression. This fact results in a huge social and emotional

impact to the families of the patients as well as an enormous financial burden to the public health systems of the so-called first world countries, where these diseases are more prevalent [58, 59]. Thereby, in the last two decades, several authors created transgenic and Knock-in mice with the purpose of testing more effective therapeutic strategies that might be translated into the clinic. The efforts of these authors are described in the following chapter together with a comprehensive comparison of their models, based on the motor impairments and neuropathology, highlighting the main advantages and disadvantages of each one.

SCA2 mouse models

The following models will be discussed chronologically according to their publication year, consisting of 4 transgenic and 1 Knock-in (KI) mice: Q58 [60]; Q75 [61]; Q42KI [62]; Q127 [63]; BAC-Q72 [64].

Q58

This is the first report of a mouse model of SCA2, where the authors created a transgenic line that expresses a full length version of the human ATXN2, with 58 'CAG's [60]. This mutant gene is regulated by a heterologous promoter (Purkinje cell protein 2 – Pcp2) that directs the expression of the transgene to the PCs of the mice, which are the primary targets of degeneration in this disease. The authors used the hybrid B6D2F1 as the genetic background for both the model and the control group, which expresses the cDNA of the human ataxin-2 with 22 glutamines (Q22). The most characterized mouse line was the Q58-11, which incorporated three copies of the human transgene, contrary to the Q22 lines, with just one copy. After confirming the expression of the mutant protein in the *cerebellum* of the transgenic mice, the authors characterized these animals using a panel of behavioral tests that included clasping, footprinting and rotarod.

Motor impairments

The mice expressing the mutant ATXN2 exhibited clasping at 8 months of age, contrary to the control group (Q22). Also, the same animals showed a 19% reduction in the stride length at 16 weeks of age, when compared with the control and the WT. Likewise, the rotarod test showed a significant worse performance for the homozygous Q58 when comparing with the control group and the WT, with a smaller latency to fall (around 50%)

at the 16 weeks of age. These motor deficits were progressive, with both the homozygous and the heterozygous Q58 showing severe impairment at 26 weeks of age. There were no differences detected between the Q22 lines and the WT, in any of the tests. In a subsequent characterization done by Liu and co-workers [65], a general lack of balance and coordination was reported in the Q58 mice, as measured by the beam walk test, when comparing with WT mice. These differences became significant at 8 months of age, including longer latencies to cross the beam and an increased number of foot slips, which worsened in a progressive manner with aging.

Neuropathology

The neuropathology in this model showed a decrease in the immunoreactivity with Calbindin-28K - a marker for neuronal dysfunction – at four weeks of age for the homozygous Q58. Similarly to the motor dysfunction, the loss of Calbindin-28K was progressive and worsened from 7-14 weeks. At 24-27 weeks of age, the authors also detected a significant loss of 50% in the number of PCs in the mutant lines, contrasting with the control lines that showed no signs of neuropathology at any time point. In a different work [66], these Q58 transgenic mice were further characterized and an abnormal electrophysiological profile of these cells was reported at 24 weeks, worsening in a progressive manner with aging. This profile includes a decrease in the number of firing PCs and a reduced firing frequency of PCs in SCA2 mice, when compared with the WT.

Overview

The Q58 transgenic mice have a very well-characterized ataxic phenotype and neuropathology as its greatest advantages. In fact, these mice exhibit not only a strong motor impairment in the rotarod, but they are also the only described model with a reported ataxic gait, lack of balance and clasping. Besides that, they have a marked neuropathological phenotype, being the only SCA2 mice with clear signs of neuronal dysfunction, neuronal loss, ataxin-2 aggregates and electrophysiological dysfunctions in PCs.

This severe and demarked phenotype makes this mouse model appropriate to study the effect of new therapeutic strategies in different aspects of the SCA2 phenotype, as it was demonstrated already by some interesting works: in 2009, Liu and co-workers [65] treated the Q58 mice with a pharmacological inhibitor of the Ryanodine receptor, successfully improving the performance of the mutant animals in the beam walk and the rotarod, and

establishing this receptor as a potential therapeutic target for SCA2; Chang and colleagues, in 2011 [67], rescued some of the Q58 motor symptoms by injecting these mice intravenously with human mesenchymal stem cells; in 2012, Kasumu and co-workers [68] used a selective modulator of the SK2/3 channels, administered orally, to alleviate the motor dysfunctions of this model, achieving a significant improvement in the beamwalk and accelerated rotarod; on a different work, Kasumu and colleagues [66] relied on a phosphatase, delivered by adeno-associated viruses, to inhibit the 1,4,5-triphosphate receptor-mediated calcium release. This strategy was successful in preventing the PC dysfunction and rescuing some of the motor impairments of the SCA2 mice. Besides this importance for therapy the Q58 transgenic mice are the only ones, together with the Q127, that have reported electrophysiological impairments in the PCs, which make them appealing for the study of PCs degeneration in SCA2 (table 2).

Nevertheless, there are some issues worth of notice in this model. First, it uses a heterologous promoter that, unlike the human patients that have expression of mutant ATXN2 across the whole body, directs the expression exclusively to the PCs. This feature, although useful for the study of cerebellar dysfunctions, makes the analysis of other brain regions, such as the *striatum* and *substantia nigra*, virtually impossible. Second, the method of pronuclear injection by which this model was generated results in the integration of the transgene in a random location of the genome, which might be disrupting the function of endogenous genes. Finally, the three Q58 founder mice integrated two, three or four copies of the transgene, leading to expression levels that might not be physiological (table 2).

Q75

Another model was developed in 2006, when Aguiar and colleagues [61] used the same methodology of pronuclear microinjection to create a mouse model with a human full-length version of the ATXN2. The human gene was isolated from a Cuban patient with 75CAG using RT-PCR and obtaining an amplicon of 4.477 Kb corresponding to the cDNA of the ataxin-2 isoform 1. This transgene was then expressed in the transgenic model under the regulation of the self human SCA2 promoter. This approach allowed obtaining ubiquitous expression of the transgene across the entire body of the animal, as it was detected at the transcript level in the lungs, kidney, muscle tissue, brain and liver, and at the protein level in the *cerebellum*. The authors used the mouse hybrid strain B6D2F1 X OF1 as the genetic background for this model, and as a control strain for the behavioral

tests, WT littermates. F066, that integrated one or two copies of the SCA2 transgene, was the most characterized line.

Motor impairments

An ataxic behavior was observed in the Q75 mice when subjected to the rotarod assay. Indeed, a significant worse performance by the heterozygous transgenic animals was observed at 12 weeks, and by the homozygous at 6 weeks of age, when compared with the WT.

Neuropathology

Interestingly, the neuropathology revealed that, despite the ubiquitous expression throughout the body, only the PCs showed signs of degeneration, exhibiting a somewhat targeted effect.

Overview

The Q75 model has an increased biological relevance when comparing with the Q58 since it exhibits the expression of the transgene in several tissues across the whole body. Moreover, these mice display a severe motor impairment, with an earlier onset of those symptoms than any other model. This rapid disease progression makes the Q75 mice more suitable and affordable to test new therapies and assess its effects in the motor coordination and neuropathology (table 2).

The major disadvantages lie with the method of pronuclear injection that promotes random integration, and also to the lack of a transgenic animal line with wild-type ATXN2, to serve as a suitable control. Although the motor incoordination is quite severe, there is no information available of any other behavior and the neuropathology is not as well characterized as in the Q127 or in the Q58 (table 2).

Q42KI

The first and only report so far of a knock-in mouse model of SCA2 was published in 2012, by Damrath and colleagues [62]. In this work, the authors used the basic concept of the homologous recombination in embryonic stem cells to replace the normal murine atxn2 gene with a mutagenized version with 42CAG repeats. This mutant form is under the control of the endogenous murine atxn2 promoter and was transmitted stably to the progeny for over nine consecutive generations. Moreover, the gene product was detected in the

cortex and *cerebellum* at the transcript and protein level, demonstrating that the 'CAG' expansion does not impair the atxn2 transcription and translation. The C57BL/6 mice strain was used as the genetic background and the WT littermates served as the controls for phenotypic evaluation.

Motor impairments

The mutant mice exhibited a very mild ataxic behavior: no differences were found in the open field, grip or footprint analysis between the Knock-ins and the WT. As for the accelerating rotarod, the differences became significant only at 18 months of age, for the homozygous mice. On its turn, the heterozygous didn't show any impairment at all when compared with the WT, at any time point analyzed.

Neuropathology

The neuropathological assessment also revealed very mild and late-onset alterations, consistent with the behavioral results. In fact, the only perceptible alterations were cytoplasmic ataxin-2-containing insoluble aggregates, identified in the PCs of the Knock-in mice. These aggregates first became detectable at 14 months of age, and then at 24 months in much higher number. There were no signs of neuronal loss, neurodegeneration or nuclear inclusion bodies.

Overview

By analyzing the phenotype of these Knock-ins, Damrath and co-workers detected a significant 19% reduction in the weight of these animals as early as 10 days of age, when comparing with the WT group. This significant difference remained for their entire life and serves as an extra piece of evidence for the role of ataxin-2 in metabolism and body weight, which will be discussed in more detail in the discussion.

Contrasting with every other model, the Q42KI mice present a faint and very late-onset phenotype, probably due to the reduced number of 'CAG's. Indeed, although they have a reduced body weight starting in the first week of age, the first behavioral symptoms appear at 18 months, with a mild impairment in motor coordination, and only for the homozygous animals. Likewise, the only neuropathological hallmarks detected were the presence of cytoplasmic ataxin-2 aggregates, at 56 weeks. This makes up the biggest disadvantages for this model, especially for research into new therapeutic strategies, where a strong and early-onset ataxia is preferable. Also, the heterozygous Q42KI did not show any motor

impairment when compared with the WT, contrary to what happens in human SCA2 patients (table 2).

Notwithstanding this, a huge advantage comes to mind in this model, which is its faithfulness to the human condition: physiological levels of expression, targeted insertion, and a very late onset of the symptoms. This makes it suitable to study the very early molecular mechanisms involved in the pathology of SCA2. The authors of this work did exactly that, by performing a genome-wide transcriptomic analysis in the *cerebellum*, brain stem and liver of the Knock-in and the WT mice, and identifying one gene – Cyp4a14, involved in cholesterol biosynthesis - differentially expressed in the liver at 6 months of age. In a subsequent study in 2016, Halbach and colleagues [69] investigated the cerebellar transcriptome of these Q42KI, finding deregulated expression levels of two genes involved in calcium homeostasis. Indeed, Atp2a2 and Itpr1 transcripts appear to be downregulated in the *cerebellum* of the Q42KI mice as well as in a SCA2 KO mice [49], giving strength to the hypothesis that deranged calcium signaling is a fundamental process in the PCs degeneration found in the Q58 and the Q127 model [65]. These experiments are in accordance with similar studies in HD [70] and MJD [71] and demonstrate the importance and applicability of this model, which might reveal new insights into the early mechanisms of SCA2 and identify new therapeutic targets (table 2).

Q127

Another transgenic mouse model was created in 2013 [63] with a slightly different objective and thereby a distinct approach. The purpose was to evaluate the electrophysiological and gene expression changes in PCs in SCA2, and to correlate those variations with the onset of the motor phenotype. With this objective in mind, Hansen and co-workers created a mouse model with 127 ‘CAG’ repeats under the Pcp2 promoter to obtain a strong and targeted degeneration in the PCs as well as a robust ataxic phenotype. The authors used the mouse strain B6D2F1 as the genetic background for this model and, as a control strain for the behavioral tests, WT littermates were used.

Motor impairments

As early as 8 weeks was enough to show a motor dysfunction in the accelerating rotarod in the transgenic mice, which worsened in a progressive manner until 36 weeks of age. By this time point, the latency to fall of the mutant animals showed a significant reduction of 50% when compared with the WT littermates.

Neuropathology

The neuropathology of the Q127 mice was also altered, with the presence of ataxin-2 aggregates in the PCs at 4 weeks, and increasing in number in subsequent time points. Another important feature was the decrease in the molecular layer thickness, which became significant at 12 weeks of age and progressively aggravated, becoming over 60% reduced comparing with the WT littermates. Neuronal loss was also observed in the transgenic animals, at 40 weeks of age, with a reduction in the number of PCs. Finally, the electrophysiological profile of these cells also showed differences in the mutant animals, namely a slower firing frequency that was significant at 6 weeks and worsened with age.

Overview

The Q127 transgenic shows a very robust and well-characterized phenotype, with an early-onset severe dysfunction in the motor coordination of these mice and a well-studied neuropathology including an evaluation of the electrophysiological impairments in the PCs. This particular feature is an important new insight that has only been reported in the Q58 model before. Indeed, an electrophysiological profile of SCA2 had been made in several studies involving human patients [72, 73], but the recording of firing patterns in PCs is not possible in humans for obvious reasons. All in all, these features make the Q127 animals quite suitable for testing therapeutic strategies and also to study the electrophysiology of SCA2 Purkinje neurons (table 2).

The biggest disadvantage of this model, to our understanding, lies with aspects that confer low biological relevance when comparing with the Q42KI or the BAC-Q72: a targeted expression of the mutant ataxin-2 to the PCs; the very high number of 'CAG's, which is rarely found in the population; the method of pronuclear injection; and the lack of a transgenic animal line with wild-type ATXN2, to serve as a suitable control (table 2).

BAC-Q72

Finally, in 2015, Dansithong and co-workers developed the most recent transgenic mouse model of SCA2 available, with 72 'CAG' repeats [64]. This model was created with Bacterial Artificial Chromosomes (BAC), which are DNA constructs based on a functional fertility plasmid (or F-plasmid). In recent years, these large-insert DNA clones have been used to create transgenic animals mainly due to its capacity to include an entire gene

sequence, including non-coding regions [74, 75]. This feature should allow the transcription, by alternative splicing, of both isoforms of ataxin-2 although there was no reference to this topic in the publication. As for the genetic background, the authors used the FVB mouse strain for both the model and the control group, which contains the entire gene of the human ATXN2 with 22 'CAG's (BAC-Q22). Also, the BAC-Q72 and the BAC-Q22 integrated 4 and 10 copies of the corresponding transgenes, respectively, and the endogenous human promoter regulates them both. This strategy allowed obtaining ubiquitous expression of the transgenes across the entire body of the animal, as it was detected at the transcript level in the heart, liver, and the entire central nervous system (CNS) and at the protein level in the *cerebellum*. The most characterized mutant line was the BAC-ATXN2-Q72.

Motor impairments

The transgenic with the mutant ataxin-2 suffered impairments in the motor coordination, showing a decreased latency to fall in the accelerating rotarod, which started at 16 weeks of age and progressively worsened until the 36 weeks.

Neuropathology

The neuropathological analysis also showed dysfunctions in these BAC-Q72 mice, at 24 months of age, with loss of the calbindin and Pcp2 proteins in the *cerebellum*.

Overview

The most recent transgenic model of SCA2 presents a new approach, which is the use of the BACs to insert the mutant ATXN2 transgene. This strategy has been used to create some very robust models of disease [76, 77] and its advantages include the insertion of the entire gene sequence into the host genome. This constitutes an important breakthrough since it allows for the normal splicing events and the regulation by non-coding regions of ATXN2 to take place. Together with the more physiological levels of transgene expression that are obtained, these aspects make the BAC-transgenic models very reliable and faithful to the human condition. In addition to this, the ataxic behavior had a sooner onset and was more pronounced than the Q42KI, which combines two desirable characteristics to test for new therapies in a single SCA2 model (table 2).

Interestingly, both the BAC-Q72 and the BAC-Q22 also weighted significantly less than the WT, starting at 8 weeks of age and progressing until a 30% reduction when comparing

to the WT littermates. Once again, this topic will be explored with further detail in the discussion, but this result reinforces the role that ataxin-2 plays in metabolism and body weight.

As disadvantages, we refer to the very mild neuropathology and to the lack of other behavior/symptoms, such as clasping or ataxic gait (table 2). Given its characteristics, this model might also be suitable to unravel the role of the different isoforms of ataxin-2 in the pathophysiology of SCA2, a topic that is still poorly understood.

To conclude, all the transgenic/Knock-in mouse models of SCA2 have advantages and disadvantages, which we summarized in table 2, taking into account all the main features of the models in a global perspective. Nevertheless, all of them have proven very useful to the understanding of this terrible neurodegenerative disease. Indeed, some of these models are extremely faithful to the human condition, especially the most recent ones like the BAC-Q72 transgenic or the Q42KI, with physiological levels of expression and a late onset of symptoms. On the other hand, the other transgenic mice (Q58, Q75 and Q127) might lack some biological relevance, but became extremely powerful tools to investigate new therapeutic strategies, possessing robust phenotypes and early onset of symptoms.

As it was mentioned before, other cellular and animal models of SCA2 have been made, appart from the transgenic and KI mice here described in detail. These other models include experiments done in *S. cerevisiae* [44, 46, 78], *C. elegans* [42, 43] and *D. melanogaster* [45, 79], as well as a celular model derived from human induced pluripotent stem cells [80] and two KO mice [47, 49]. These studies have provided an invaluable insight into the pathways regulated by ataxin-2 and its role in the disease progression, with some of them helping to understand and explain many results obtained in our own model.

Despite the high quality and useful SCA2 mouse models created so far, there are other modeling strategies that have never been used for this disease, such as the viral-based overexpression of ataxin-2, which presents some advantages over the transgenic and Knock-in mice. As a matter of fact, this kind of strategy is quite useful to generate robust and long-term expression of the transgenes in well-defined regions of the brain. This allows to study the specific contribution of each brain region to the whole disease process, without the interference of other sectors. It also allows to test different variations of the transgene, such as truncated, full-length, WT or mutant ATXN2 (with variable number of 'CAG's), as well as different mammalian species like nonhuman primates.

Table 2 – The major advantages and downsides of SCA2 mouse models

Mouse models	*Representative line*	*Advantages*	*Disadvantages*
Q58	Q58-11	Robust, well-characterized behavioral impairments and neuropathology; Suitable to study PCs degeneration; Suitable for research into new therapeutic strategies;	Unable to study other brain regions: targeted expression to PCs; Non-physiological expression levels of ataxin-2; Pronuclear injection: random integration;
Q75	F066	Ubiquitous expression of mutant ataxin-2; Integrated only 1 or 2 copies of the transgene; Early onset of symptoms and robust motor impairment – suitable to test for new therapies;	Pronuclear injection: random integration; Lack of control transgenic line; No other symptom besides motor incoordination;
Q42 KI	CAG42	Very faithful to the human condition in terms of physiological expression levels and age of onset; Ideal to study early differential gene expression levels; Targeted insertion;	Mild ataxia phenotype with late onset of symptoms; Mild neuropathology with late onset of symptoms; Unsuitable to test new therapies that alleviate symptoms;
Q127	$ATXN2^{Q127}$	Very robust impairments in behavior with early onset of symptoms; Very robust neuropathology with early onset of symptoms; Suitable to study electrophysiological dysfunctions in PCs and new therapies;	Unable to study other brain regions: targeted expression to PCs; Non-physiological number of CAG repeats – 127Q; Pronuclear injection: random integration;
BAC-Q72	BAC-ATXN2-Q72	The entire gene (introns included) was inserted into the mouse genome; More physiological levels of ataxin-2 expression; Ubiquitous expression of mutant ataxin-2;	No other symptoms besides motor incoordination; Very mild neuropathology;

The SCA2 mouse models created so far have focused mainly on the *cerebelllum*, leaving other brain regions with a well-described neuropathology (in autopsies of human patients) generally unexplored. Based on the viral-based approach previously described, we aimed to study the contribution of the *striatum* to the pathophysiology of SCA2 and hopefully

create a relatively cheap and quick model to easily evaluate new therapeutic options. Indeed, not only has the *striatum* been reported to show mutant ataxin-2 inclusions [33, 38] and neurodegeneration [26], but the high frequency of parkinsonism in SCA2 patients also suggests that the role of this brain region in the disease might be more important than what was first thought.

Objectives

The global objective of this work was to investigate the specific contribution of the *striatum* to the pathophysiology of SCA2, concerning a wide range of neuropathological features and behavioral alterations.

The specified objectives were:

- To investigate the propensity of mutant ataxin-2 to aggregate in the *striatum.*
- To ascertain whether the overexpression of mutant ataxin-2 induced neuronal dysfunction in the *striatum*.
- To research the effects of overexpressing mutant ataxin-2 in striatal neuroinflammation.
- To evaluate the implications of overexpressing mutant ataxin-2 in striatal synaptic components.
- To assess whether the overexpression of mutant ataxin-2 in the *striatum* induced cognitive or metabolic alterations.

Chapter II – Materials and Methods

Lentiviral vectors

The cDNAs encoding for human full-length wild-type ataxin-2 (ATXN2-22CAG), and mutant ataxin-2 (ATXN2-104CAG) were kindly provided by Prof. Stephan Pulst and cloned in a self-inactivating (SIN) lentiviral vector under the regulation of the Phosphoglycerate Kinase 1 (PGK) housekeeping promoter, as described previously [81]. Each one of these plasmids were transfected into human embryonic kidney (HEK) 293T cells for lentiviral particles production, using a four plasmid system described previously [82]. The lentiviral particles were produced and resuspended in 0.1M phosphate-buffered saline (PBS) with 0.5% Bovine Serum Albumin (BSA). Viral titer was assessed by measuring HIV-1 p24 antigen content through an enzyme-linked immunosorbent assay, which estimates the number of p24 positive particles per µl of solution (ng/ µl) (RETROtek, Gentaur, Belgium). Viral stocks were stored at -80 ºC until use.

Animals

8-week-old C57/BL6 male mice (Charles River) were used in this experiment. The animals were housed in a temperature controlled room maintained on a 12h light/ 12h dark cycle. Food and water were provided *ad libitum*. The experiments were carried out in accordance with the European Community directive (86/609/EEC) for the care and use of laboratory animals.

Stereotaxic injections in the *striatum*

Concentrated viral stocks were thawed on ice and resuspended by repeated pipetting. For the bilateral injections, lentiviral vectors encoding for mutant ataxin-2 (ATXN2-104CAG) were stereotaxically injected into the right hemisphere of the striatum in the following coordinates: antero-posterior: +0.6mm; lateral; +1.8mm; ventral: -3.3mm; mouth bar: 0. As an internal control, the left side of the *striatum* was injected with lentiviral particles encoding for WT ataxin-2 (ATXN2-22CAG) in the following coordinates: antero-posterior: +0.6mm; lateral; -1.8mm; ventral: -3.3mm; mouth bar: 0. The animals were anesthetized by administration of a mixture of ketamine (100mg/kg, Clorketam 1000,

Vétaquinol) with xylazine (10mg/kg, Rompun®, Bayer) by intraperitoneal injection (ip). A single 2 µl injection of 400'000 ng viral particles was injected on each hemisphere at a rate of 0.25 µl/min by means of an automatic injector (Stoelting Co., Wood Dale, IL, USA) through a 34-gauge blunt-tip needle linked to a Hamilton syringe (Hamilton, Reno, NV, USA). After injection, the syringe needle was elevated for 0.2 mm and left in place for an additional 5 min to maximize the viral vector diffusion and to minimize backflow. As for the unilateral injections, only the right side of the striatum was injected with 500'000 ng of lentiviral vectors (adjusted for 2µl of volume) encoding for either mutant or WT ataxin-2. Mice were kept in their home cages for 8 weeks before being sacrificed.

Tissue preparation

Animals were sacrificed by sodium pentobarbital overdose, transcardially perfused with 0.1 M phosphate buffer solution and a 4% paraformaldehyde fixative solution (Fluka, Sigma) followed by brain removal. The brains were post-fixed in 4% paraformaldehyde for 24 h and later incubated in 20% sucrose/phosphate buffer for 48 h. The brains were then frozen at -80 ºC and coronal slices of 25 µm were sectioned using a cryostat (LEICA CM3050 S). Slices were collected and stored in 48 multi-well plates, free-floating in 0.1 M phosphate buffer solution supplemented with 0.12 mmol/L sodium azide. The plates were kept at 4°C until their posterior analysis by either fluorescence or light immunohistochemistry.

For western-blot and qRT-PCR purposes, animals were sacrificed by sodium pentobarbital overdose and the brains were directly removed without perfusion. Brains were dissected fresh and the whole *striatum* was removed and frozen at -80 ºC until further processing. For posterior analysis, the whole *striatum* of each mouse was cut in half, with one of the parts being used for total RNA extraction and the other one for total protein extraction.

Immunohistochemistry

The immunohistochemical procedure for light microscopy was initiated by incubating free-floating sections for 30 min at 37ºC in phenylhydrazine diluted in 0.1 M phosphate buffer solution (1:1000) to inhibit endogenous peroxidases. The sections were then incubated at

RT for 1h in a blocking solution containing 0.1% Triton X-100 and 10% Normal Goat Serum (NGS, Gibco) in PBS, to block non-specific interactions of the antibody and preventing background staining. The same blocking solution was used to dilute the appropriate primary antibodies: anti-ubiquitin (Rabbit, 1:300; Enzo), anti-DARPP-32 (Rabbit, 1:1000, Millipore), anti-ataxin-2 (Rabbit, 1:500, Millipore). These incubations were performed over-night at 4ºC. A biotinylated secondary antibody (anti-rabbit, 1:200, Vector Laboratories) diluted in blocking solution was used to incubate the sections at RT for 2h, followed by an amplification step. This was done by a reaction with the Vectastain ABC kit (Vector Laboratories, West Grove, USA). To visualize bound antibodies, the free-floating sections were incubated with 3,3'-diaminobenzidine substrate (Vector Laboratories, West Grove, USA) that is oxidized and acquires a brown color in the presence of the peroxidase-bound antibodies. Incubation was performed for a maximum of 5 minutes to avoid excessive background staining, after which the sections were mounted on microscope slides. Before the final step of cover slipping with Eukitt® (O. Kindler GmbH & CO, Freiburg, Germany) as a mounting medium, the tissue was first hydrated for 30 s, followed by 4 subsequent steps of complete dehydration. This was achieved by incubating the sections in solutions with an increased percentage of ethanol (EtOH 75%, 96%, 100%) and a xylene substitute solution (Sigma) for 3 min each. The coverslipped microscope slides were then allowed to dry in a fume hood for 24 h. Images were acquired in a Zeiss open-field PALM Microbeam imaging microscope (Carl Zeiss Microimaging, Germany), equipped with AxioCam HR colour digital cameras (Carl Zeiss Microimaging) using a 5x and 20x Plan-Neofluar objectives (0.25 and 0.4 numerical amplitude, respectively).

For the fluorescence immunohistochemistry, an initial blocking step was done by incubating the sections with a solution containing 0.1% Triton X-100 and 10% Normal Goat Serum (NGS, Gibco) in PBS for 1h at RT. This same blocking solution was then used to dilute the appropriate primary antibodies: anti-IBA-1 (rabbit, 1:250, Wako), anti -GFAP (rabbit, 1:1000, DAKO), anti-VGLUT (guinea-pig, 1:1000, Millipore), anti-synaptophysin (rabbit, 1:1000, Millipore). These incubations were performed over-night at 4ºC, except for the incubation with anti- VGLUT which was done for 72 h at 4ºC. The correspondent secondary antibody was also diluted in blocking solution (anti-rabbit, anti-mouse, 1:200; anti-guinea pig, 1:500 Alexa Fluor®, Invitrogen) and was coupled to a fluorophore (either 488, 594 or 647 nm). The sections were incubated in this solution for 2h at RT, except for the staining of VGLUT which was left over-night at 4ºC. After a washing step, the sections

were mounted on microscope slides and coverslipped with the Mowiol mounting medium. The visualization of the fluorescent sections required 3 different microscopes, depending on the experiment. The staining of Iba-1 and GFAP were visualized in the Zeiss open-field PALM Microbeam imaging microscope (Carl Zeiss Microimaging, Germany), equipped with AxioCam HR colour digital cameras (Carl Zeiss Microimaging) using a 5x and 20x Plan-Neofluar objectives (0.25 and 0.4 numerical amplitude, respectively). The staining of VGLUT was visualized on a Zeiss Axio Observer Z1 microscope (CCD digital Axiocam HRm camera; ZEN Blue software; Carl Zeiss AG, Oberkochen, Germany) with a 63x oil objective (Plan-Apochromat, 1.4 numerical amplitude). One field per section was analyzed, in a total of 6 sections per animal (n=3). The staining of synaptophysin (SYP) was visualized in a laser scanning confocal microscope Zeiss LSM 510 Meta (Carl Zeiss Microscopy) using the blue (405nm) and green (488nm) lasers and a 63x oil immersion objective. A total of 3 sections per animal (n=4) were scanned, with 3 different fields per section imaged using the LSM 510 META software. All fluorescence parameters were maintained constant to enable sample comparison. The 3 referred microscopes use the ZEN digital imaging software package (Carl Zeiss Microimaging).

Quantification using the CellProfiler software

The sections stained for ataxin-2 were analyzed using the CellProfiler software [83], which allows to measure the mean and maximum intensity of ataxin-2 staining, exclusively on the transduced cells. After introducing a series of parameters (intensity, size, shape, texture) as thresholds, which we defined as transduced cells, the software scans the black and white images for these parameters and automatically converts them into a system of colors. These colors indicate the intensity displayed by each cell expressing exogenous ataxin-2, which is demonstrated in the supplementary figures S2A-C, as an example. The fluorescent images of SYP and VGLUT staining were also analyzed with this software, calculating the number of *puncta* and their intensity. All quantifications were performed with the same settings for each measurement and using CellProfiler's object identification modules.

Quantification of the neuroinflammatory response

The sections stained for GFAP and Iba-1 were analyzed with the ImageJ software package (Image J software, USA). The "area" and the "intensity per area" of astrogliosis was quantified by delineating the area of activation of GFAP-positive "activated" astrocytes close to the injection site, and then measuring the immunoreactivity within that area. The intensity for Iba-1-positive "reactive" microglia was quantified by measuring the immunoreactivity displayed throughout the entire image.

Evaluation of the extent of DARPP-32 depleted volume

The extent of either the ATXN2WT or ATXN2MUT lesions in the striatum was analyzed by photographing, with a 5x objective, 8 DARPP-32 stained sections per animal (25 µm thickness sections at 200 µm intervals), specifically selected to acquire the complete rostro-caudal sampling of the striatum. For each of the sections, the lesioned area was quantified with the Image J software (Image J software, USA) and then extrapolated into the lesioned volume by applying the following equation: volume = $d*(a1+a2+a3…a8)$, where d is the distance between subsequent sections (200 µm) and $a1+a2+a3…a8$ are DARPP-32 depleted areas for individual sections.

Behavioral assessment

For the assessment of mice exploratory behavior and motor horizontal activity, open field tests were performed in an activity cage (Panlab, Barcelona, Spain). Mice were placed in a 50×50 cm arena with 50 cm-high walls and their movement activity was recorded for 40 min using the Acti-Track System (Panlab, Barcelona, Spain). The collected data were analyzed for the first 10 min in the arena and for the last 30 min. The statistical analysis was performed by multiple student's t-test using the GraphPad software (La Jolla, USA).
The cognitive behavior was evaluated through an adapted T-maze test described previously [84]. Briefly, each animal was left to walk and freely explore the arena for 10 min, to minimize the "exploratory effect" during the actual test. This habituation day was done 3 times with one week interval between them, before the 8th week (when the behavioral

assessment was performed). The test was separated in a "learning day" and a "switch task day". The first consisted in 8 trials, each one of them composed by a forced and a free choice. In the forced step, one arm of the arena was obstructed and the mice were therefore compelled to enter the only accessible one, which had a food reward and a visual cue (white rectangle attached to the wall). After a 10 min resting break, the free choice part was conducted, which is equal to the forced part with the exception that both arms of the maze were available. The mice were thereby trained to turn in the same direction as the forced part. No more than two consecutive turns in the same direction were allowed, and the animals were left in the maze until they found the reward, up to a maximum of 5 min (for the forced and the free choice steps). See supplementary figure S2D for a schematic representation.

Finally, the switch task day consisted of 18 free choice trials, where the white rectangle was the only indication of the "correct answer". Likewise, an equal number of turns to the left and to the right were required, and no more than two consecutive turns in the same direction were allowed.

All behavioral tests were performed in a dark room after at least 1h acclimatization.

Quantitative real-time PCR

Total RNA was extracted from the *striatum* with the Nucleospin RNA kit (Macherey-Nagel) according to the manufacturer's instructions, after a first step of dissociating the tissue with Trizol (TRI reagent, sigma) and chloroform. The RNA concentration and purity were determined with NanoDropTM 2000 (Thermo Scientific). After RNA quantification, 1 μg of total RNA was converted into cDNA using iScript cDNA synthesis kit (Bio-Rad, Hercules, CA), in a Veriti 96-well thermocycler (Applied Biosystems). RNA extraction and cDNA synthesis for mRNA quantification were performed following the manufacturer's instructions. Quantitative RT-PCR was performed using SsoAdvanced™ Universal SYBR® Green Supermix (Bio-Rad), in a Step One Plus Real-Time PCR System from Applied Biosystems. The primers used were the following (all mouse): IL-1 Beta (QT01048355); HPRT (QT00166768); SQSTM1/P62 (QT00127855); PABP (QT01673315); Beclin-1 (QT00139006); all pre-designed (QuantiTect Primer Assays, Qiagen); and EIF4E: Forward (5'-GCTCTATACAACCATATCCAG-3'), Reverse (5'-AATCCCGTCCTTAAAAAGTG–3') EIF3E: Forward (5'–CAATGTGTCCACATA-

TTCTACG-3'), Reverse (5'–GTGTAAGACTCCTGTTGAATC–3'); RPL14: Forward (5'-AAATTGATGCCAGAGAAAGG-3'), Reverse (5'–CTGTTCCTCATTTTCTTTGC–3'); GADPH: Forward (5'–TGGAGAAACCTGCCAAGTATGA-3'), Reverse (5'–GGTCCTCAGTGTAGCCCAAG–3'); Dlg4/PSD-95 (ref NM_001109752) from Sigma; and CD11B: Forward (5'- TCGCTACGTAATTGGGGTGG-3'), Reverse (5'-TAGATGCGATGGTGTCGAGC-3') from Invitrogen; Briefly, 2.5 µl of the cDNA obtained in the reverse transcription reaction diluted 10-fold with DNase free deionized water were used. The quantitative PCR was performed as follows: one single cycle at 95 ºC for 30 s, followed by 45 cycles of two steps: first step of 5 s at 95 ºC, second step of 15 s at 57 ºC (for EIF4E, EIF3E and RPL14) or at 58 ºC (for CD11B) or at 60 ºC (for the remaining genes). The melting curve protocol started immediately after the quantitative PCR and consisted of 5 s heating at 65 ºC with a 0.5 ºC temperature increase in each step until 95 ºC was reached. The threshold cycle (Ct) values were generated automatically by the StepOneTM Software (Applied Biosystems). To each gene, and in each experiment, a standard curve was performed and quantitative PCR efficiency was determined by the software. The geneX program (version 4.1.7, MultiD Analyses) was used to choose the most adequate reference genes for normalization. We uploaded a list of 18 duplicate Ct values for HPRT, GADPH and EIF4E and used both the GeNorm [85] and the NormFinder [86] software (included in geneX) to choose the best reference genes. These two published and validated algorithms function by analyzing the stability among samples and experimental conditions, and they both identified EIF4E and GADPH as the most suitable reference genes (see figs S2E and S2F). Based on these results, each target gene was normalized to these two housekeepings and the values of the mice injected with ATXN2MUT were compared to those injected with ATXN2WT.

Western-blot

For the protein extraction protocol, striatal tissue was liquefied and lysed in Radio-Immunoprecipitation Assay (RIPA) buffer 3540 solution (50mM Tris HCl, pH 8, 150nM NaCl, 1% NP-40, 0.5% sodium deoxycholate, 0.1% sodium dodecyl sulphate) containing proteases inhibitors (Roche diagnostics GmbH) followed by 3 series of 4-s ultra-sound pulse (1 pulse/s). Total protein lysates were stored at -80ºC, and protein concentration was determined with the Pierce™ BCA Protein Assay Kit (Thermo). 60 µg of protein extract

were resolved in sodium dodecyl sulphate-polyacrylamide gels (4% stacking, 10% resolving), transferred onto PVDF (polyvinylidene fluoride) membranes. The membranes were blocked by incubation in 5% non-fat milk powder or 5% BSA in 0.1% Tween 20 in Tris buffered saline (TBS-T) for 1h at room temperature. Immunoblotting was performed using the following antibodies: anti-ataxin-2 (rabbit, 1:500, Millipore), anti-GFAP (rabbit, 1:1000, DAKO), anti-Calreticulin (rabbit, 1:1000, abcam), anti-PSD-95 (rabbit, 1:1000, Cell signaling), anti-GM130 (rabbit, 1:1000, Abcam), anti-Synaptophysin (rabbit, 1:1000, Millipore), anti-SQSTM/P62 (rabbit, 1:1000, Abgent). Incubations with the primary antibodies were performed over-night at 4ºC followed by incubation with the anti-rabbit alkaline phosphatase-linked secondary antibody for 2h at RT. Bands were visualized with Enhanced Chemifluorescence substrate (ECF, GE Healthcare) and chemi-fluorescence imaging (VersaDoc Imaging System Model 3000, Bio-Rad). One of the membranes was normalized to soluble human ataxin-2 and the other 2 were normalized to DARPP32 levels. DARPP32 was chosen for normalization upon confirming that its levels remained overall unchanged (fig. S2G). Densitometric analysis was carried out in the same gel using ImageJ software (Image J software, USA).

Statistical analysis

Statistical analysis was performed using the GraphPad software (La Jolla, USA) to identify outliers (Grubbs test with $\alpha = 0.05$) or significant differences between two groups (paired Student's t-test for the immunohistochemistry images; unpaired Student's t-test for the behavioral analysis, qPCR and western-blot). Statistical differences are considered either significant (* $p<0.05$, ** $p<0.01$, *** $p<0.001$) or non-significant (ns). All the quantifications were made by the same operator, blindly.

Chapter III - Results

Striatal bilateral injection of lentiviruses encoding for ATXN2WT or ATXN2MUT induces widespread transduction levels and significant differences in neuropathology features

The high tropism for neurons and long-term stable expression of transgenes by the SIN-W lentiviral vectors has been well demonstrated in previous studies [87, 88]. Therefore, they have been extensively used in CNS diseases modeling, due to their ability to overexpress a mutated gene in specific parts of the brain, allowing for a more targeted study of those traits [89, 90]. Moreover, this strategy has been particularly successful in modelling HD and MJD in the *striatum*, creating very useful and reproducible models to understand disease progression and evaluate new therapeutic strategies [82, 91]. These reasons led us to choose this vector to study the involvement of the *striatum* in SCA2 and hopefully establish a new animal model of this trait. The ~4200 bp cDNA of human ATXN2 either with 22CAG (WT gene) or 104CAG (mutant gene) was successfully cloned in the SIN-W lentiviral vector under the regulation of the Phosphoglycerate Kinase 1 (PGK) promoter and the lentiviral vectors were produced (fig. 3A). The stereotactic injections were performed bilaterally in 8 C57BL/6 mice, so that the left side of the *striatum* overexpressed ATXN2WT to serve as an internal control for the right side, overexpressing ATXN2MUT.

The animals were perfused and sacrificed at 8 weeks post-injection and their brains removed for further processing (see materials and methods). The light immunohistochemical analysis of the tissue revealed a widely dispersed expression of Ataxin-2 in both sides of the *striatum* (fig. S1A) although displaying a very distinct pattern between the WT and the mutant hemisphere (fig. 3B). In order to quantify this difference, a series of 8 sections per animal were scanned with the CellProfiler software [92], which we used to count all the transfected cells for each image and then determine the mean and the maximum intensity displayed by those cells. Both these measurements presented a statistically significant increase in the side injected with ATXN2MUT, when comparing with the control side (fig. 3C), suggesting that the mutated form of ataxin-2 accumulates abnormally in the *striatum*. Surprisingly, staining with an antibody against ubiquitin did not reveal any inclusion, neither nuclear nor cytoplasmic, and therefore no differences between the two hemispheres (fig. 3D). This result suggests that the accumulated species of mutant ataxin-2 might be degraded by an ubiquitin-independent selective autophagy process.

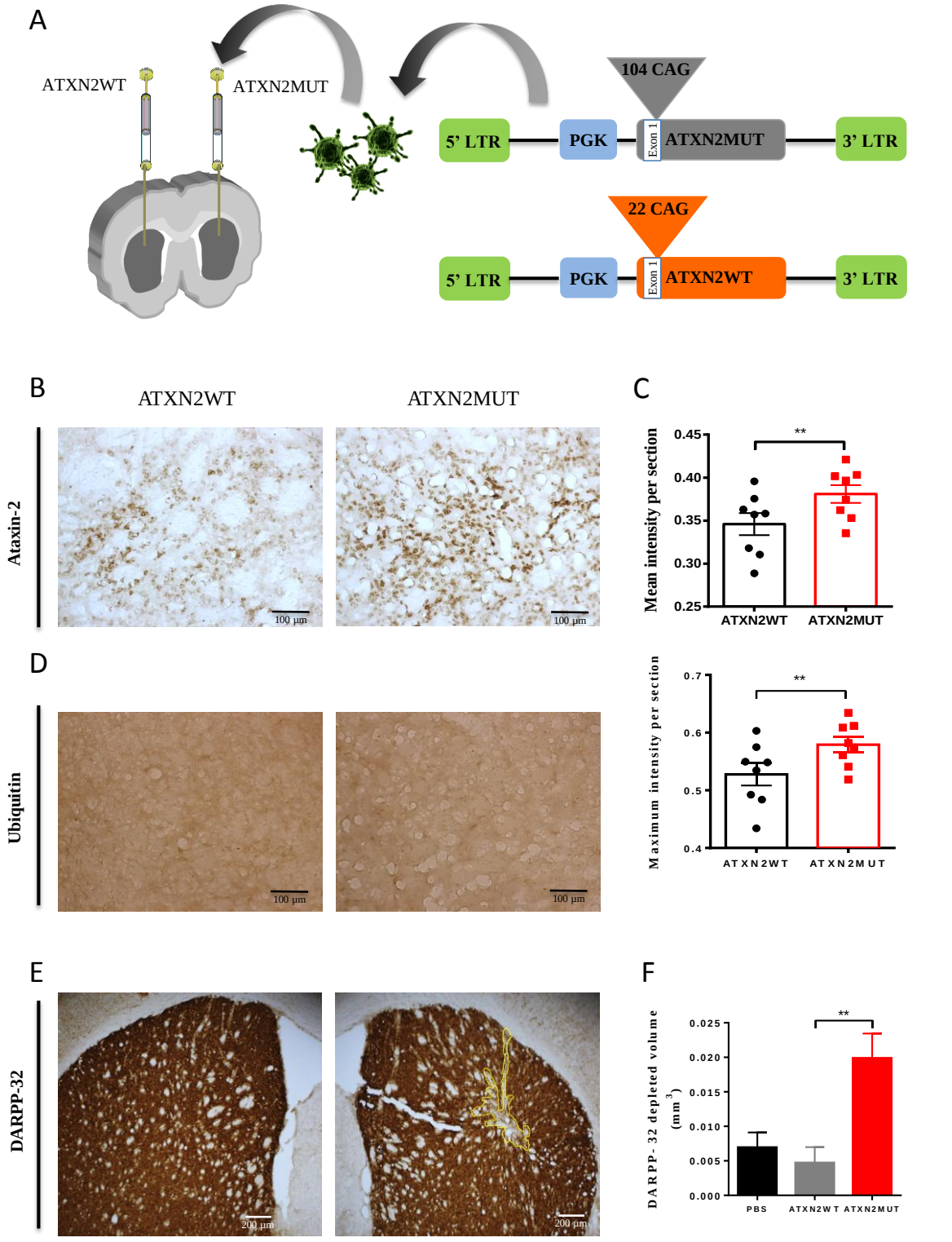

Figure 3. The overexpression of the mutant form of Ataxin-2 induces the formation of non-ubiquitinated high molecular weight species and DARPP-32 loss in the *striatum*. (A) Representative outline of the experiment. ATXN2WT with 22CAG and ATXN2MUT with 104CAG were cloned in the SIN-PGK lentiviral backbone and transfected into HEK293T cells to produce lentiviruses (see materials and

methods). Viruses encoding for ATXN2WT were injected in the left side of the striatum to serve as a control to the right side, injected with ATXN2MUT. **(B and C)** The cells transduced with the mutant form of the protein displayed a significantly higher intensity, on average per section, and also higher maximum levels per section when compared to the ones transduced with the WT form. The results were obtained with the CellProfiler software, using 8 sections of each bilaterally injected animal (n=8). **(D)** Staining with an anti-ubiquitin antibody revealed no ubiquitinated inclusions on either side of the *striatum* (n=4). **(E and F)** The side of the *striatum* that was injected with ATXN2MUT presented a significantly higher neuronal dysfunction than the side injected with either ATXN2WT or PBS. A total of 8 sections from 8 bilaterally injected animals (n=8) were stained with an anti-DARPP32 antibody and the lesion area was quantified with the ImageJ software. Data is presented as mean ± SEM. **$p<0.01$, paired student's t-test.

In order to explore whether the mutant protein induced neuronal dysfunction, we used an antibody against DARPP32, whose staining delineates the *striatum* perfectly and facilitates the visualization of lesions. Indeed, similarly to other striatal models of disease [82, 91, 93] the expression of the mutant form of ataxin-2 induced a lesion in the area stained for DARPP32, which was quantified with the ImageJ software [94] (figs. 3E and 3F).
So, the injection of ATXN2MUT in the *striatum* did not produce ubiquitinated inclusions of the mutant protein but induced neuronal dysfunction, when compared with the control hemisphere (injected with ATXN2WT).

Striatal injection of lentiviruses encoding for ATXN2MUT does not trigger neuroinflammation but leads to moderate synaptic dysfunction

With the purpose of assembling a more complete picture of the neuropathological alterations induced by ATXN2MUT, we performed a series of fluorescent immunohistochemical staining's. We began by looking into neuroinflammation, since it plays a decisive role in several neurodegenerative disorders, sometimes even in pre-symptomatic stages, through the activation of astrocytes and microglia [95].
Despite this fact, we found no differences in the area of astrogliosis between both sides of the *striatum* (figs. 4B and S2A). Instead, the hemisphere that overexpressed the mutant protein revealed a slight decrease in the staining of GFAP, a cytoskeletal constituent of astrocytes, when comparing with the side that overexpressed ATXN2WT (n=4). This tendency was quantified by delineating the area of activation of astrocytes close to the injection site, using the ImageJ software, and then measuring the immunoreactivity within

that area (figs. 4B and 4C). The immunoreactivity given by Iba-1 was also quantified but presented no differences between the mutant hemisphere and the control one, suggesting that there is no activation of microglia (figs 4B and 4D).

The effect of mutant ataxin-2 in synapses was investigated by staining with antibodies against the pre-synaptic protein Synaptophysin and the glutamate transporter VGLUT. For synaptophysin, confocal images were taken from 3 different fields per section, using 3 sections per animal in a total of 4 bilaterally injected mice (n=4) and then these images were analyzed using the CellProfiler software [92]. Both the number of SYP puncta and their mean intensity per field per section, appear to be significantly reduced in the hemispheres overexpressing mutant ataxin-2 (figs. 4B, 4E and 4F). As for the VGLUT staining, 6 sections per animal were analyzed, in a total of 3 bilaterally injected mice (n=3). There is a tendency for a decreased number of *puncta* in the hemisphere overexpressing mutant ataxin-2, when comparing with the side expressing the WT form of the protein (figs. 4B and 4G). Although this difference is not significant, these are not confocal images and only 1 field per section was analyzed. Considering this, it is our belief that a greater number of fields and a greater number of animals analyzed on a confocal microscope might have rendered a more robust difference.

In conclusion, the overexpression of mutant ataxin-2 in the *striatum* does not trigger a neuroinflammatory response but it induces several synaptic alterations, significantly decreasing the number of puncta of synaptophysin and a tendency for decreasing the number of *puncta* of the glutamate transporter VGLUT.

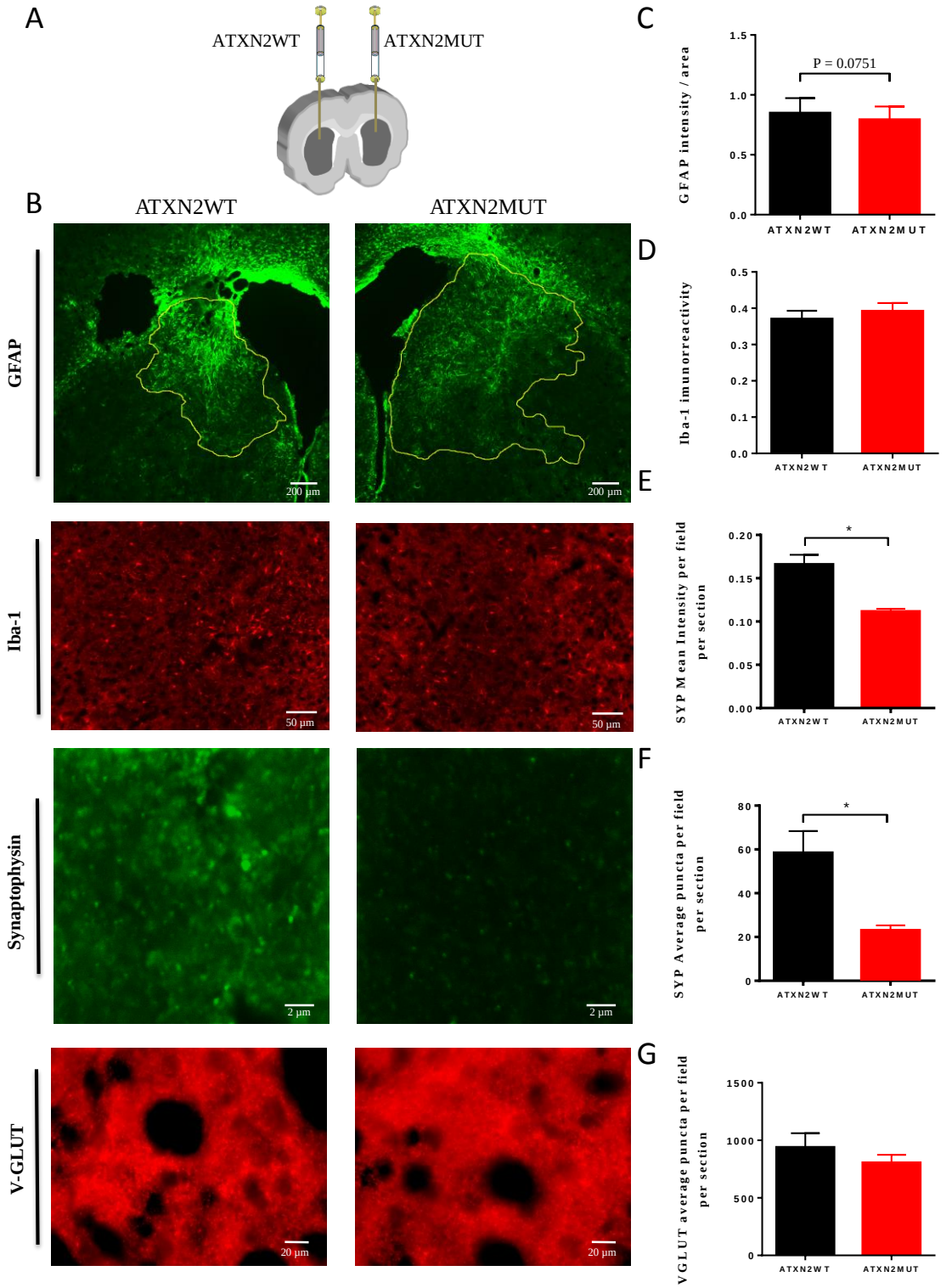

Figure 4. Mutant Ataxin-2 decreases astrocytic activation and causes a moderate dysfunction of synapses in the *striatum*. (A) Schematic representation of the bilateral injection for this experiment. WT animals were injected with ATXN2WT in the left side of the *striatum* and ATXN2MUT in the right side. **(B)** Representative images of the WT and mutant side, stained with GFAP (upper panel), Iba-1 (second panel),

Synaptophysin (third panel) and VGLUT (lower panel). For each staining, the representative image consists of the mutant side and the respective WT control. **(C)** The hemisphere of the *striatum* that overexpresses the mutant protein shows a decreased immunoreactivity for GFAP within the area of astrocytic activation, when compared with the control hemisphere. A total of 8 sections from 4 bilaterally injected mice were used (n=4) and quantified with the ImageJ software. **(D)** The Iba-1 immunoreactivity didn't show any differences between the WT and the mutant side of the *striatum* (n=4). **(E)** Both the mean intensity and the number of *puncta* **(F)** of synaptophysin are significantly decreased in each field analyzed of the mutant side of the *striatum*, when compared with the control. A total of 4 animals (n=4), 3 sections per animal and 3 fields per section were analyzed and quantified in the CellProfiler software. **(G)** There is a tendency for a decrease in the number of *puncta* in the VGLUT staining for the hemisphere that overexpresses mutant ataxin-2, when comparing with the control side. A total of 3 animal (n=3), 6 sections per animal and 1 field per section were analyzed and quantified in the CellProfiler software. Data is presented as mean ± SEM. *$p<0.05$, paired student's t-test.

Striatal unilateral injection of lentiviruses encoding for ATXN2MUT results in hyperactivity, reduced anxiety and ipsilateral turning behavior

Given the previous results that indicated synaptic alterations in the *striatum* upon injection of ATXN2MUT, we wanted to investigate what implications this could have in the behavior. Indeed, the role of ataxin-2 in metabolism and obesity has been well-documented before – driven from the two KO models [47, 49] and the Q42KI model [62] – and the importance of the dorsolateral striatum in cognitive behavior, especially in habit learning processes is also well-established [84, 96]. Considering these facts, we had good reasons to suspect a behavioral phenotype would arise from the ATXN2MUT-injected animals.

In order to investigate this, we performed a new set of experiments that included the unilateral injection of C57BL/6 mice with lentiviruses encoding for ATXN2WT (n=9) or ATXN2MUT (n=9) in the right side of the *striatum*. During the 8th week post-injection, these animals together with 5 WT mice were tested in the open field to uncover any alterations in the metabolism or anxiety and were also tested in an adapted T-maze, to explore the existence of cognitive impairments. The most striking conclusion is that the group injected with ATXN2MUT presented a hyperactive behavior, when compared with both the WT and the group injected with ATXN2WT. Indeed, the mutant mice systematically covered higher distances in all time points and zones analyzed (figs. 5B, 5F and S3A-D) and performed a higher number of rearings than the control groups (fig. 5E), clearly demonstrating a hyperactive exploratory behavior.

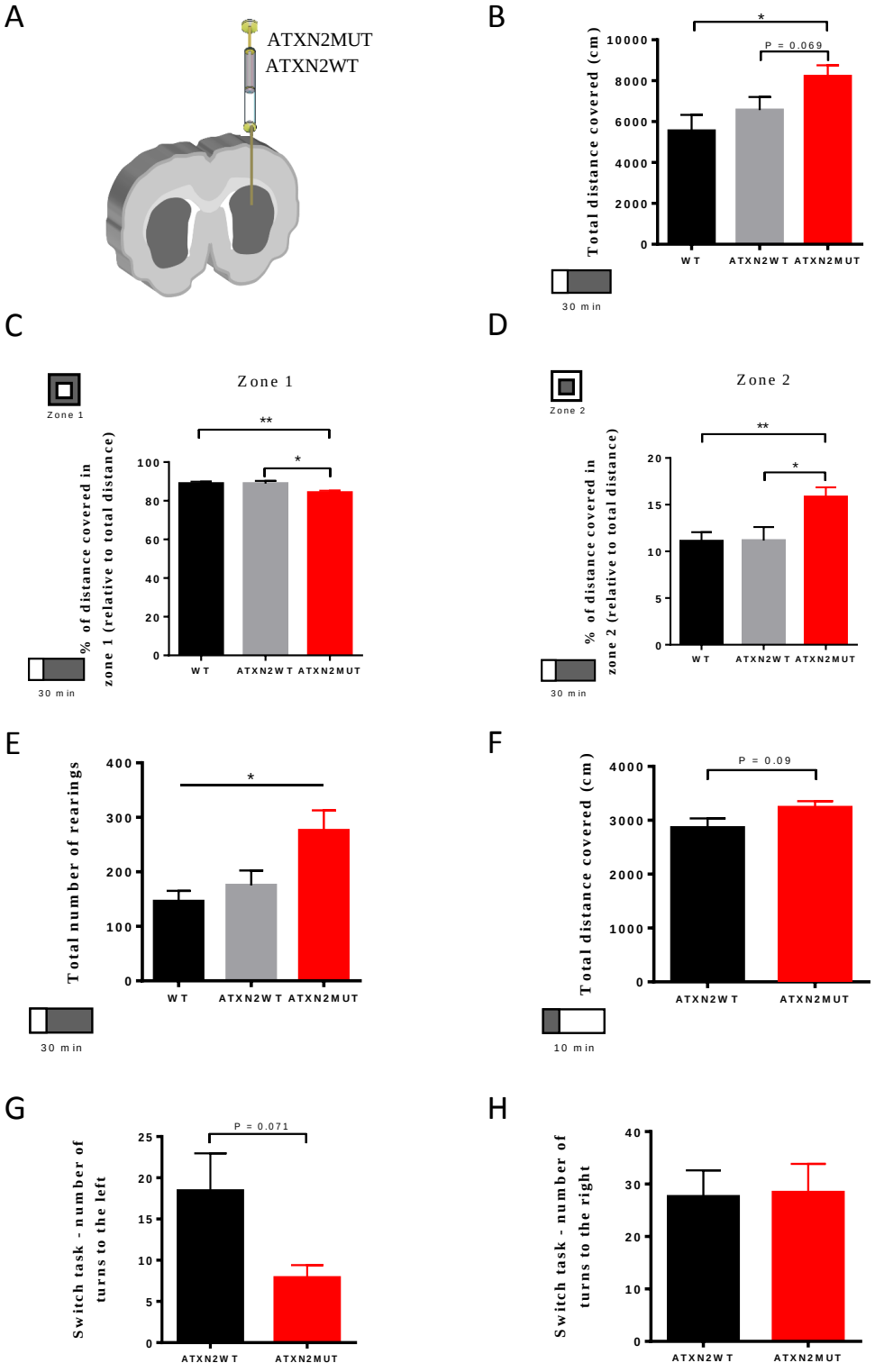

Figure 5. The injection of ATXN2MUT in the right side of the *striatum* induces a hyperactive behavior, as well as decreased anxiety and ipsilateral turning behavior. (A) Schematic representation of the unilateral injections for this experiment. WT animals were injected either with ATXN2WT or ATXN2MUT in the right side of the *striatum*. **(B)** The mice expressing mutant ataxin-2 (n=8) tended to cover longer

distances in the final 30 min of the open field test, when compared to the animals expressing WT ataxin-2 (n=9) and significantly longer comparing with their WT littermates (n=5). **(C and D)** The animals that overexpressed the mutant form of the protein preferred the central area of the open field (Zone 2) instead of the periphery (Zone 1), as indicated by the distance traveled in each zone relative to the total distance **(E)** The mice injected with ATXN2MUT (n=8) had an increased exploratory behavior indicated by a significantly increased number of rearings, when compared with both the WT (n=5) and the animals injected with ATXN2WT (n=9). **(F)** When analyzing only the first 10 min of the task, again there was a tendency for mutant mice to cover longer distances then their control counterparts. **(G)** In the Switch task day of the T-maze test, the animals expressing mutant ataxin-2 (n=5) showed a strong tendency to fail such test, when it involved turning to the left side of the maze while turning to the right **(H)** did not show any differences between these and the mice expressing ATXN2WT (n=4). Data is presented as mean ± SEM. *$p<0.05$, **$p<0.01$, unpaired student's t-test.

A different illation to be drawn from these behavioral tests is a reduced anxiety exhibited by the animals overexpressing mutant ataxin-2. In fact, while the WT and the group overexpressing WT ataxin-2 preferred to walk by the peripheries and corners, that is believed to give the animals a sense of protection, the mutant mice demonstrated to be more fearless and prone to explore the central area of the activity box (figs 5C and 5D). We also analyzed the first 10 minutes of habituation to the task, but found no significant differences, except for a consistent tendency to travel longer distances (figs. 5F, S3C and S3D).

The T-maze test was performed on a smaller number of animals to allow for a bigger number of trials: 5 mice injected with ATXN2MUT and 4 mice injected with ATXN2WT. The task was divided in two different days: the habituation day, intended for learning, consisted of 8 trials; and the Switch task day consisted in 18 trials. Although there were no differences in habit-learning ability (figs. S3E and S3F), the test revealed a very strong tendency towards an ipsilateral turning behavior of the mutant mice. In fact, whenever the "correct" answer consisted in turning left, the mice overexpressing mutant ataxin-2 failed considerably more than the control group (fig. 5G). However, when the "correct" answer required turning to the right side, there were no differences between the two groups (fig. 5H).

To summarize, the overexpression of the mutated form of ataxin-2 in the striatum of mice induces hyperactive exploratory activity and dissociated fear/ reduced anxiety. Another effect is an abnormal turning behavior to the ipsilateral side of the injection.

Striatal unilateral injection of lentiviruses encoding for ATXN2MUT alters the expression levels of genes involved in synaptic activity, autophagy, and the regulation of translation

It is fairly consensual that in many neurodegenerative diseases, alterations in mRNA levels can occur in very early stages of the disease and often precede the appearance of the first symptoms [97]. The Q42KI model starts showing the first ataxic symptoms at 18 months of age, but as early as 6 weeks of age is enough to display dysregulated mRNA levels [62, 69]. Considering the lack of ubiquitinated aggregates of mutant ataxin-2 in the *striatum*, the modest degeneration shown by the staining with DARPP32 and the synaptic dysfunction of this striatal model, we set out to measure the expression levels of particular genes related with: autophagy (Beclin-1 and P62), inflammation (IL-1 Beta and CD11B), synaptic activity (PSD-95) and the regulation of translation (EIF3E, PABP, RPL14). We expected to get a more precise picture of the transcriptomic changes in the *striatum* of SCA2, in an early stage of disease, and shine some light over previous results.

With this purpose in mind, the unilaterally injected mice of the previous experiments were sacrificed by the end of the 8th week post-injection, and the total mRNA was extracted and converted into cDNA (see materials and methods). We used quantitative real-time PCR to compare the gene expression values from mice overexpressing WT ataxin-2 with the group overexpressing the mutated form. The mRNA levels of the post-synaptic protein PSD-95 were significantly increased in the mutant group, suggesting some sort of compensation mechanism to the dysfunctions in synapses (fig. 6B). Also, the injection of ATXN2MUT in the *striatum* apparently dysregulates the expression levels of genes involved in translation, as can be seen by a strong tendency to increased levels of RPL14 and a significant increase in the levels of PABP (fig. 6C). We also found evidence for the upregulation of P62 and Beclin-1 (fig. 6D), two genes involved in autophagy, which gives us a clue about the degradation pathway of the accumulated mutant ataxin-2, quantified in the figure 3C. Finally, the unaltered expression levels of CD11B and the minor tendency for upregulation of IL-1 Beta was in agreement with the general lack of a neuroinflammatory response depicted in figure 4.

To sum up, the animals injected with ATXN2MUT in the *striatum* have upregulated expression levels of PSD-95 and Beclin-1 and tendencies for P62 and RPL14. On its turn, the PABP gene is downregulated, demonstrating that the overexpression of mutant ataxin-2

is interfering directly with the cellular mechanisms of autophagy, synaptic activity and regulation of translation.

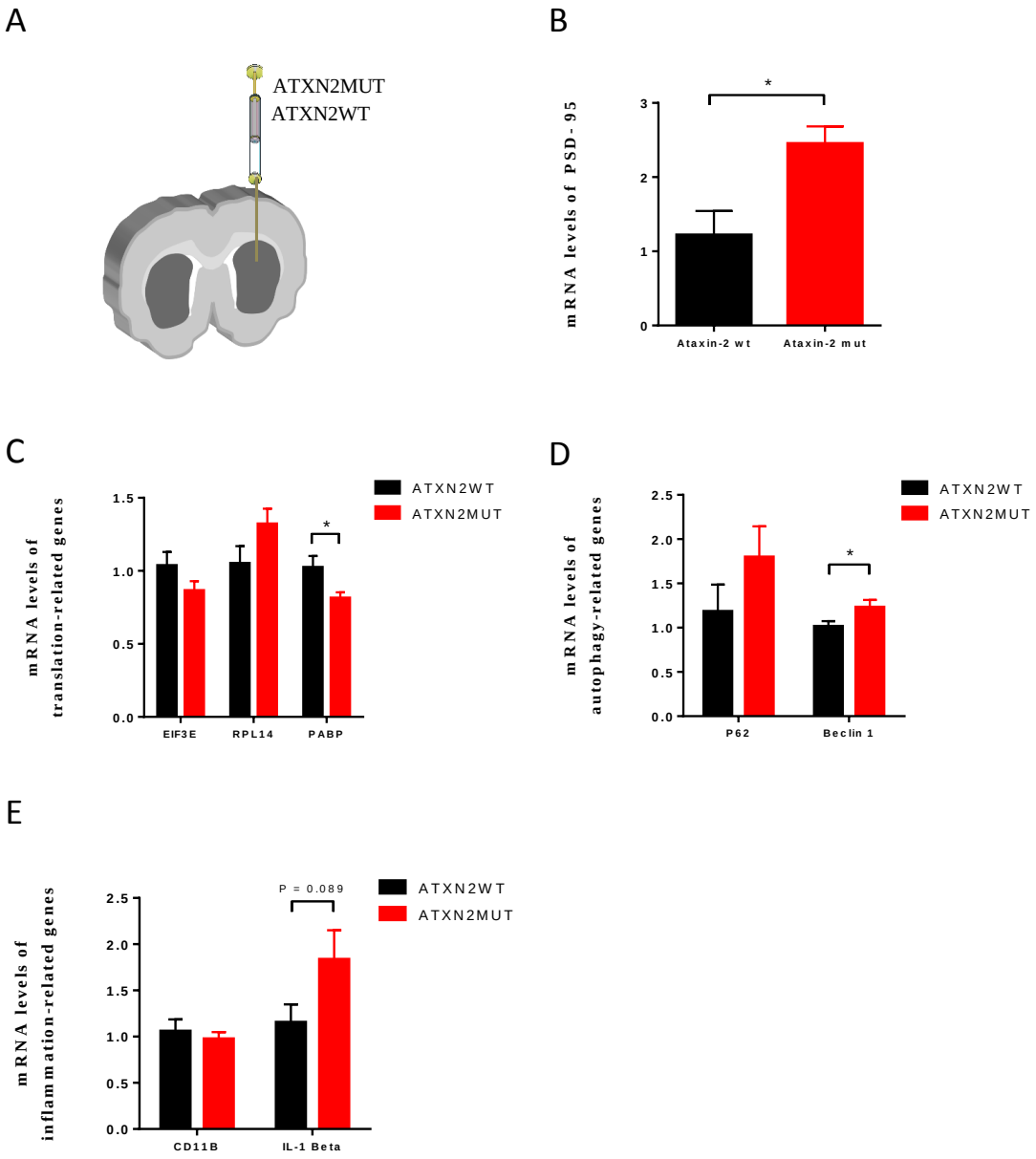

Figure 6. The injection of ATXN2MUT in the right side of the *striatum* induces a series of alterations at the mRNA level of genes involved in synaptic activity, autophagy and the regulation of translation. **(A)** Schematic representation of the unilateral injections for this experiment. WT animals were injected either with ATXN2WT or ATXN2MUT in the right side of the *striatum*. **(B)** The mRNA levels of PSD-95 were significantly increased in the animals injected with ATXN2MUT (n=8), as opposed to those injected with ATXN2WT (n=7). **(C)** The mice expressing mutant ataxin-2 presented dysregulated mRNA levels of genes involved in the regulation of translation, including tendencies for EIF3E and RPL14 and reaching statistical significance for PABP (n=8). The values are normalized for those of the mice expressing the WT protein

(n=9). **(D)** The injection of ATXN2MUT also induced an increase in autophagy-related genes, namely in P62 (n=4) and Beclin 1 (n=8), when comparing with the injection of ATXN2WT (n=7 for P62 and n=9 for Beclin 1). **(E)** Although the expression level of the gene CD11B showed no differences whatsoever between the mutant animals (n=8) and the ones expressing WT ataxin-2 (n=9), IL-1 Beta shows a tendency to appear upregulated in the animals injected with ATXN2MUT (n=8), demonstrating an inflammatory response of some kind. All qPCR results were normalized to two housekeeping genes (EIF4E and GADPH). Data is presented as mean ± SEM. *$p<0.05$, unpaired student's t-test.

The unilateral injection of ATXN2MUT in the striatum leads to the formation of high molecular weight species and altered levels of many endogenous proteins

The same samples that were used for the mRNA extraction in the previous experiments were also processed for total protein extracts to run western-blots. The purpose was to compare protein levels of the mice expressing mutant ataxin-2 with the control group (expressing WT ataxin-2) and compare those results with those obtained in previous sections.

In a first set of experiments with 4 animals injected with ATXN2WT and 5 injected with ATXN2MUT, we began by measuring the protein levels of human ataxin-2 and those of mouse PSD-95, Calreticulin and GFAP (fig. 7A). The quantification of this blot revealed a significant increase in the high molecular weight species of ataxin-2 in the animals injected with the mutant protein. This somehow validates the results obtained in the figure 3C, confirming that the mutant form of ataxin-2 has a higher propensity to form high molecular weight species and might accumulate abnormally in striatal neurons (fig. 7B). The protein levels of PSD-95 remain unchanged (fig. 7C), despite the significant increase in the transcript levels (fig. 6B), suggesting some type of dysfunction in the translation of this mRNA. Given the previously described association of ataxin-2 with the Endoplasmic reticulum, we checked the protein levels of Calreticulin, which were significantly downregulated in the mice injected with ATXN2MUT (fig. 7D). Interestingly, the western-blot not only confirmed the lack of astrocytic activation, but also shows a strong tendency for decreased levels of GFAP in the group overexpressing the mutant protein (fig. 7E). This result was somehow unexpected and suggests some existing dysfunction in the mechanism of astrocytes activation.

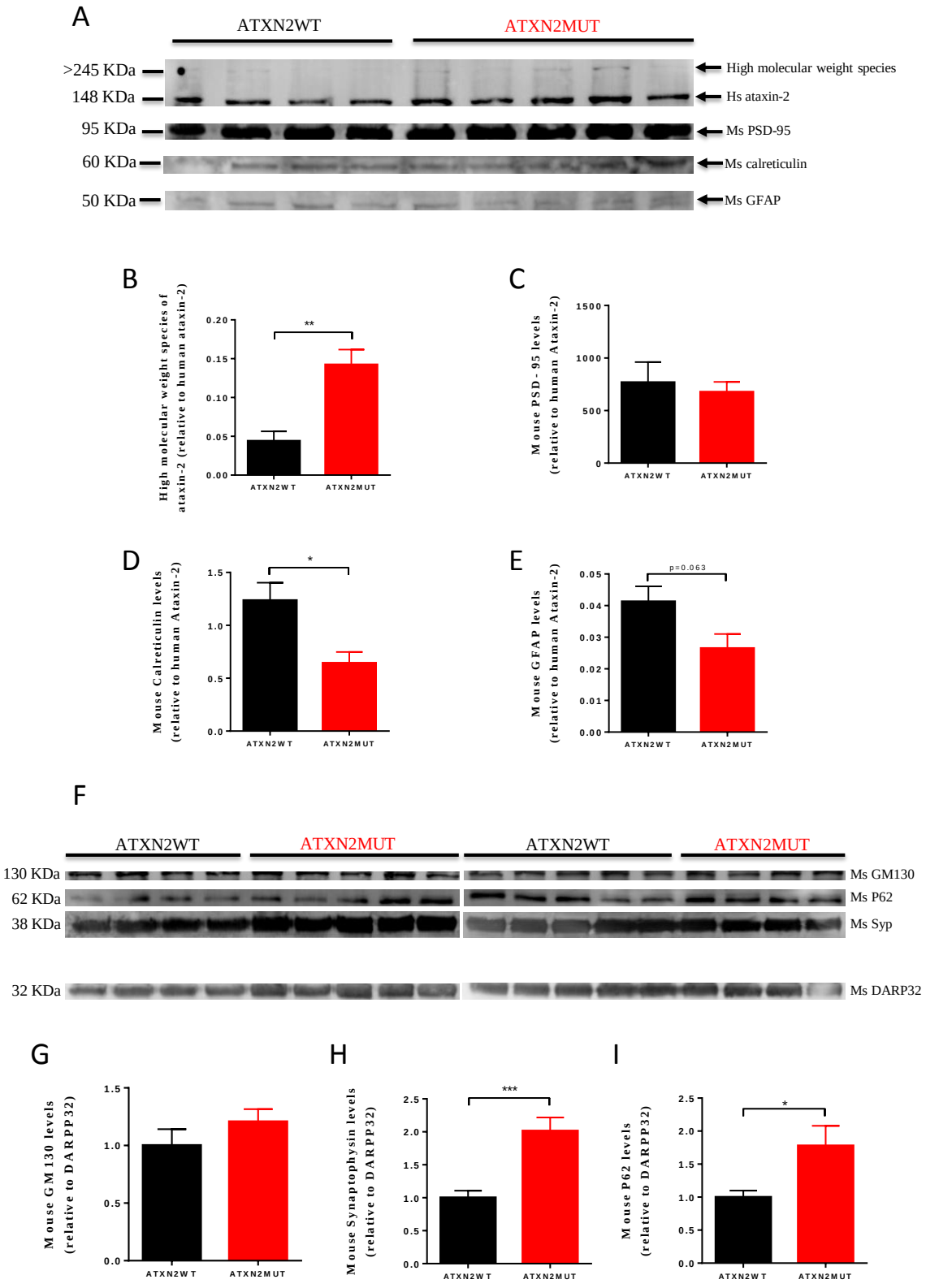

Figure 7. The overexpression of human ATXN2MUT in the *striatum* leads to the formation of high molecular weight species as well as several alterations in the levels of endogenous proteins. (A) Western-blot of the right side of the *striatum*, either injected with viruses encoding for ATXN2WT (n=4) or

ATXN2MUT (n=5). All bands of this blot were normalized to the overexpressed human Ataxin-2 (~148 KDa) **(B)** The overexpression of the mutant form of the protein leads to a significant increase in the levels of high molecular weight species, when comparing with WT form. **(C)** The protein levels of PSD-95 appear to be unchanged between animals injected with ATXN2WT or ATXN2MUT. **(D and E)** The injection of ATXN2MUT led to a significant decrease in the protein levels of both Calreticulin and GFAP, compared to the injection of ATXN2WT. **(F)** Western-blot analysis of the right side of the *striatum*, either injected with viruses encoding for ATXN2WT (n=9) or ATXN2MUT (n=9). All the bands of these blots were normalized to the protein levels of endogenous DARPP32 (~32 KDa). **(G)** The protein levels of GM130 are unaltered between animals overexpressing the mutant protein and those that overexpress the WT form. **(H and I)** Both the levels of Synaptophysin and P62 are significantly increased in the mice injected with ATXN2MUT, when comparing with the control group. All western-blot results were analyzed and quantified with the ImageLab software. Data is presented as mean ± SEM. *p<0.05, **p<0.01, ***p<0.001, unpaired student's t-test.

In a second set of experiments with 9 mice injected with ATXN2WT and 9 injected with ATXN2MUT (fig. 7F) we observed unaltered expression levels of GM130 but significantly increased levels of synaptophysin and P62 (figs. 7G-I). The detected levels for synaptophysin were somehow unexpected, taking into account the results described in figures 4E and 4F, but at the same time confirms the overall panel of total synaptic dysregulation.

To conclude, the overexpression of the mutant form of ataxin-2 in the *striatum* alters the expression levels of several endogenous proteins, similarly to what happens at the transcript level.

Chapter IV - Discussion

The purpose of this work was to develop and characterize a lentiviral-based striatal model of SCA2 in order to clarify the role of the *striatum* in the disease and hopefully serve as a platform to test new therapeutic strategies. Due to the very scarce information regarding the theme of this work, any outcome of the experiments would always be new and original. Even so, there were some unanticipated results which we will discuss in the following section along with the 3 aspects of this model that we consider to be fundamental.

Aggregation and neuronal dysfunction

This study was pioneer in clarifying that the mutated form of the protein ataxin-2 is significantly more prone to form high molecular weight species and consequently accumulate abnormally in the *striatum*. The lack of any ubiquitin-labeled inclusions (fig. 3D) was a surprising result, taking into account the results of the staining with anti-ataxin-2 (fig. 3C) and the western-blot (fig. 7B) as well as published autopsies in human patients describing striatal ubiquitinated aggregates [33, 38]. A possible explanation is that the mutant ataxin-2 is abnormally accumulated in the transfected cells but is being degraded by an ubiquitin-independent mechanism. In fact, although the majority of autophagic signals are ubiquitin-dependent, there are some cargoes delivered to the selective autophagy pathway through ubiquitin-like modifiers or lipids/sugars exposed on the cargoes [98]. In PD-related studies, some authors have shown evidence of Lewy bodies that were non-ubiquitinated and positive for the lysosomal protein LAMP-1 [99], which might strengthen this hypothesis. Besides, our own findings of significant increase in the protein levels of P62 (fig. 7I) together with upregulated mRNAs of autophagy-related genes like Beclin-1 and P62 (fig. 6D) also reinforces this theory.

Two autopsies performed in SCA2 patients have described that the staining with anti-ubiquitin antibodies revealed considerably less aggregates than staining with 1C2 (an antibody that recognizes expanded polyQ chains). This result contradicted the findings in other polyQ diseases, where inclusions are almost always ubiquitinated, and the authors theorize that this phenomena could be caused by incomplete proteolysis [33]. Also, no mouse model of SCA2 created so far ever reported the presence of ubiquitinated aggregates, and instead always relied on 1C2 or anti-ataxin-2 antibodies. For confirming or disregarding the incomplete proteolysis hypothesis, it would be interesting to perform immunohistochemistry on our striatal model and check for 1C2-positive inclusions.

Some authors studying PD have suggested a different explanation when confronted with an analogous situation of non-ubiquitinated α-synuclein inclusions. They have hypothesized that the spectrum of inclusions with variable morphology and distinct α-synuclein and ubiquitin staining that they observed, could represent different stages in Lewy bodies formation [100, 101]. According to this theory, it could be that waiting for a longer time after the injection of ATXN2MUT could have facilitated the detection of ubiquitinated ataxin-2 inclusions.

The DARPP32 protein is involved in the signaling cascades of dopamine receptors and therefore is highly concentrated in areas enriched in dopaminergic nerve terminals, such as the *striatum* and the olfactory tubercle [102, 103]. Its staining usually provides a highly reliable and quantifiable measurement of neuronal dysfunction, which can be useful to determine the ameliorating effect of new therapies. However, this type of lesion can be a reversible process, which make it tricky to analyze and highlights the importance of timings when modelling neurodegenerative diseases. Although the injection of ATXN2MUT induces a clear lesion in the DARPP32-stained area (figs. 3E and 3F), this is a very modest one when compared with previous models of striatal degeneration [82, 91, 93]. This fact, together with the total absence of ubiquitinated inclusions raises the question of whether or not 8 weeks is long enough for the maximum expression of the SCA2 phenotype in the *striatum*. This topic could be further explored in the future by performing several experiments with multiple time points post-injection.

Neuroinflammation

Another key feature of this model is the apparent lack of any mutant ataxin-2-triggered neuroinflammatory reaction, when comparing with the WT form of the protein. Due to the selectivity of the blood-brain barrier (BBB), the brain represents an immunologically-privileged site, where immune cells only enter upon a series of signaling cascades triggered mainly by astrocytes and microglia. This is the so-called neuroinflammation, which has the main purpose of fighting infections but is often responsible itself for an increased toxicity and increased neuronal loss in many neurodegenerative disorders [95]. Upon almost any kind of injury to the CNS including acute and progressive diseases [104, 105], both the astrocytes and microglia can go from a “resting” state of vigilance, into a “reactive” state, characterized by hypertrophy and overexpression of markers like GFAP (astrocytes) and Iba-1 and CD11b (microglia) [106, 107]. Although several neurodegenerative traits show

a clear neuroinflammatory response, the animal models of those diseases not always recreate this characteristic, causing uncertainty as to the exact role – beneficial or harmful – that neuroinflammation plays in neurodegeneration. Chances are that it could play a little bit of both parts, depending on the stage of the disease or the type of mutation, among other factors. A clear example is Huntington's disease, whose pre-symptomatic carriers present "reactive" astrocytes in the *striatum* while several animal models fail to do so in a convincing manner [104]. Regarding SCA2, neuroinflammation is not a striking characteristict, with little information available apart from a few studies that mention gliosis in the brains of SCA2 patients [33, 108]. None of the SCA2 mouse models created so far reported any neuroinflammation and this is in agreement with our own results that show no differences in the area of astrogliosis between both sides of the *striatum* (figs. 4B and S2A). Remarkably, the western-blot showed a strong tendency for a reduction in GFAP expression (fig. 7E), suggesting some kind of dysfunction in the ability of astrocytes to become "reactive". Nevertheless, this constitutes to be insufficient data and further studies would be needed to deepen our understanding on the subject.

Synaptic activity and behavior

The evident synaptic dysfunctions and the behavioral changes displayed by the mice injected with ATXN2MUT are also key characteristics of this SCA2 lentiviral model of the *striatum*. We discuss them together as we think the first might help to explain the second, at least in part. In fact, synaptophysin is the most abundant constituent of synaptic vesicles, and was the first one to be cloned and fully studied. Furthermore, since its expression is mostly limited to these vesicles, anti-SYP antibodies are excellent markers of pre-synaptic terminals [109]. In spite of these characteristics, the exact role of this protein in synapses remained enigmatic for a long time, especially after the first SYP KO mice were created and deemed perfectly healthy [110, 111]. However, subsequent experiments highlighted the importance of SYP in synaptic plasticity [112] and the endocytosis of synaptic vesicles [109], concluding that it plays a discrete but crucial role in normal synaptic activity. Finally, an interesting study by Schmitt and colleagues [113] reported that mice deficient in SYP exhibited an increased exploratory behavior and impaired learning and memory. The SCA2 striatal model that we present in this study shows a significant decrease in the number of SYP puncta (fig. 4F) and also an exacerbated exploratory behavior, covering significantly longer distances in the open field than the control group (figs. 5B, 5D and 5F). They also

perform a higher number of rearings, which is a good indicator of exploratory behavior (fig. 5E). In addition to all this, the mRNA levels of PSD-95, a protein that is mostly expressed in post-synaptic terminals is significantly increased (fig. 6B), which suggests a cellular compensation mechanism in response to dysfunctional synapses. Although no major conclusions can be drawn from the study of VGLUT *puncta* due to the reduced number of animals and images analyzed, there is a tendency for a decreased number of these *puncta* in the hemispheres overexpressing mutant ataxin-2 (figs. 4B and 4G). All of these results confirm the panel of synaptic alterations induced by ATXN2MUT in the *striatum* and the behavioral characteristics fit perfectly with those of Schmitt and co-workers [113].

On an interesting note, the protein levels of synaptophysin appear significantly increased in the animals injected with ATXN2MUT (fig. 7H), which is contradictory with the immunohistochemical procedures (figs. 4E and 4F). This most puzzling result seems to suggest that, despite the upregulated protein levels (fig. 7H) of this pre-synaptic protein, it is still unable to assemble functional synapses. Due to insufficient data, we could only speculate as to the reasons behind this phenomena and came out with one possible hypothesis:

Ataxin-2 has been previously implicated in the polymerization of cytoskeletal filaments of actin, studied in *D. melanogaster* [79], and it is suspected of involvement in the dynamics of tubulin as well. Based on this information, we can theorize that the mutant form of ataxin-2 interferes with the transport of synaptophysin along the axons and into the axon terminals, inducing in this way several synaptic alterations in the *striatum* and resulting in the behavioral phenotype observed.

In addition to the SYP contradictory expression levels, the protein levels of PSD-95 and GFAP also showed incongruent results, as to what was initially expected. There is a different explanation from that of the cytoskeletal dynamics that can also clarify these unexpected protein expression levels: the mRNA-binding characteristics of ataxin-2 and the role that it plays in regulating translation. Indeed, a huge number of studies explored this particular characteristic of ataxin-2 and described that: it associates with polyribosomes and localizes in the rER under normal conditions [114]; it binds to several mRNAs and translation initiation factors to stall translation under stress conditions – forming stress granules [46]; it interacts with PABP1 to regulate the initiation of translation, most likely through the binding of the former to the translation initiation factor EIF4G [115]; it modulates neurodegeneration, either enhancing [56] or ameliorating it [57]. Despite these

investigations, there are still many open questions such as the true role that ataxin-2 plays in global translation, the specific mRNAs that it binds to, or what is the real effect of the polyQ stretch in its ubiquitous function. Nevertheless, it is still quite clear that disrupting the normal function of ataxin-2 globally dysregulates the translation machinery of the cell, leading to abnormally up- and down-regulated mRNAs and proteins. Our SCA2 lentiviral model of the *striatum* shows dysregulated mRNA levels for PABP and RPL14 (fig. 5C), as well as severely decreased levels of calreticulin (fig. 7D). Taking this into account, one could hypothesize that the mutant form of ataxin-2 is toxic to the polyribosomes, as demonstrated by the decrease of calreticulin and RPL14, and downregulates RNA-binding proteins, like PABP, with a generalized dysregulation of mRNA and protein levels as a consequence.

Another important factor has to be taken under consideration when analyzing the behavior of the animals injected with ATXN2MUT. The significantly longer distances covered and the increased number of rearings performed by these mice (figs. 5B-F), when comparing with the control group, could also be interpreted as hyperactive behavior, resulting from an abnormal metabolism. In fact, weight loss is often present in many SCA2 patients, although its true causes are difficult to discern [116], and there are also reports of obesity in middle stages of the disease [117] which suggests that metabolic dysfunctions are a key characteristic of this trait. At the molecular level, ataxin-2 was implicated in metabolism and increased weight soon after the creation of the first SCA2 KO mouse model [118]. The authors of that study observed a significant weight gain in the mutant mice as soon as 3 months of age, that ended up reaching a 66% increased weight comparing with their WT littermates. Interestingly, a follow-up behavioral investigation on these mice revealed that they were hyperactive and demonstrated a reduced fear conditioning as well as impaired spatial learning [48], similarly to our own lentiviral striatal model (figs. 5B-F). The obesity phenotype was later recreated by a second KO mouse model [49] in an intriguing study where the authors hypothesized that the obesity could result from an insulin resistance phenotype, caused by a reduction of insulin receptors in the CNS and liver. In addition to this, a tissue-specific conditional Knockout of insulin receptors in rat brains surprisingly resulted in a whole-body insulin resistance phenotype and obesity [119]. By putting all of this compelling evidence together, we can formulate a different hypothesis to explain the behavior of this striatal model. Indeed, the overexpression of the mutant and therefore dysfunctional form of ataxin-2 may alter the frequency of insulin receptors in the *striatum*

with consequences in the whole-body metabolism, and leading to the observed hyperactive behavior.

On a final note, the animals injected with ATXN2MUT exhibited a biased turning behavior, while performing tasks to evaluate cognitive disabilities (figs. 5G and 5H). In fact, although the adapted T-maze test did not show any learning impairments, it was still pretty useful to display an interesting characteristic of SCA2 that was never reported in previous models of the disease: the dysfunction of the striatal dopaminergic system. When comparing with the group injected with ATXN2WT, the animals overexpressing the mutated protein showed quite a strong tendency to fail the test, whenever the correct answer required turning left (fig. 5G). This tendency was lost when the correct answer required turning to the right side (fig. 5H). The classical theories of rotating behavior state that the animal tends to turn away from the side with higher dopaminergic transmission [120, 121]. Considering that our model exhibits *ipsilateral* rotations, this would suggest that the overexpression of mutant ataxin-2 is interfering with dopaminergic signaling, probably by downregulating striatal dopamine D2 receptors and/or the dopamine transporter (DAT). Due to the insufficient data, this is merely a hypothesis, but there are some studies in humans that might reinforce this theory. For example, SCA2 was recognized as an uncommon cause of Parkinsonism, with patients responding positively to Levodopa and several authors advising for PD-diagnosed patients to be screened for genetic defects in the ATXN2 gene [122, 123]. The link between SCA2 and the impairment of the nigrostriatal dopaminergic signaling was explored in subsequent studies [124, 125] but was never, to the best of our knowledge, documented in any of the mouse models described so far.

Taking all these considerations into account, we believe that this work covers many features of SCA2, including aggregation and neuronal dysfunction measured through the staining with ataxin-2 and DARPP32, respectively. But most of all, this model shows promise by allowing the research of poorly-studied characteristics of the disease like the synaptic dysfunctions, the altered metabolism/cognition and the parkinsonism frequently observed in the human patients.

Chapter V – Conclusions and future perspectives

In this work, we used lentiviral-mediated overexpression of mutant ataxin-2 as a strategy to model SCA2 in the *striatum*, and uncover the contribution of this brain region to the overall disease process. From the subsequent characterization, we have provided strong evidence that mutant ataxin-2 accumulates abnormally in striatal neurons, but does not form ubiquitinated inclusions. Taking into consideration the high number of 'CAG' repeats used, we also show in a conclusive way that ubiquitination seems not to be a key feature in SCA2 and that it is not causal/significant to neuropathology. Indeed, we have demonstrated that non-ubiquitinated mutant ataxin-2 induces neuronal dysfunction and significant alterations in synapses in the *striatum*, with behavioral alterations as a consequence. Although the cognitive abilities seem to remain unchanged, there is a significant hyperactivity and/or increased exploratory behavior as well as decreased anxiety exhibited by these mice that fit within previous reports of SCA2 mouse models. Finally, a completely new characteristic was observed in this model, which is a biased turning behavior, possibly indicating a dysregulation of dopaminergic signaling. This possible explanation remains purely hypothetical, but whatever the cause for this behavior is, it could only have been possible to observe through a unilateral injection of the mutant protein, thus reinforcing the importance and usefulness of this striatal model.

Nevertheless, there are still many dots that need connecting in this work, for which reason it would be critical to, in the future:

- Investigate the mechanism of degradation behind this severely mutated form of ataxin-2. To this end, several immunohistochemistry assays should be performed in striatal sections, staining for 1C2, P62, Beclin-1, among others.
- Investigate the reason behind the biased turning behavior, and how it could relate to the Parkinsonism symptoms observed in many human SCA2 patients. A staining of striatal sections for the DAT should be performed, since it has been described to be downregulated in the *striatum* of patients, and also for dopamine receptors. In addition to this, the injection of lentiviral vectors encoding for mutant ataxin-2 in the *substantia nigra* could also be a future experiment to help clarifying this subject.
- Further explore the incongruent results found in neuroinflammation by repeating the immunohistochemical staining for GFAP in a larger number of sections and for the entire cohort of animals

Chapter VI - References

References

1. Fu YH, Kuhl DP, Pizzuti A, et al. (1991) Variation of the CGG repeat at the fragile X site results in genetic instability: resolution of the Sherman paradox. Cell 67:1047–58.
2. Fu YH, Pizzuti A, Fenwick RG, et al. (1992) An unstable triplet repeat in a gene related to myotonic muscular dystrophy. Science 255:1256–8.
3. Pearson CE, Nichol Edamura K, Cleary JD (2005) Repeat instability: mechanisms of dynamic mutations. Nat Rev Genet 6:729–42. doi: 10.1038/nrg1689
4. Orr HT, Zoghbi HY (2007) Trinucleotide repeat disorders. Annu Rev Neurosci 30:575–621. doi: 10.1146/annurev.neuro.29.051605.113042
5. Das Bhowmik A, Rangaswamaiah S, Srinivas G, Dalal AB (2015) Molecular genetic analysis of trinucleotide repeat disorders (TRDs) in Indian population and application of repeat primed PCR. Eur J Med Genet 58:160–7. doi: 10.1016/j.ejmg.2014.12.010
6. Fan H-C, Ho L-I, Chi C-S, et al. (2014) Polyglutamine (PolyQ) diseases: genetics to treatments. Cell Transplant 23:441–58. doi: 10.3727/096368914X678454
7. Bauer PO, Nukina N (2009) The pathogenic mechanisms of polyglutamine diseases and current therapeutic strategies. J Neurochem 110:1737–65. doi: 10.1111/j.1471-4159.2009.06302.x
8. Maas RPPWM, van Gaalen J, Klockgether T, van de Warrenburg BPC (2015) The preclinical stage of spinocerebellar ataxias. Neurology. doi: 10.1212/WNL.0000000000001711
9. Rossi M, Perez-Lloret S, Doldan L, et al. (2014) Autosomal dominant cerebellar ataxias: a systematic review of clinical features. Eur J Neurol 21:607–15.
10. Hekman KE, Gomez CM (2015) The autosomal dominant spinocerebellar ataxias: emerging mechanistic themes suggest pervasive Purkinje cell vulnerability. J Neurol Neurosur Ps 86:554–561. doi: 10.1136/jnnp-2014-308421
11. Rolim L, Leite A, Lêdo S, et al. (2006) Psychological aspects of pre-symptomatic testing for Machado-Joseph disease and familial amyloid polyneuropathy type I. Clin Genet 69:297–305. doi: 10.1111/j.1399-0004.2006.00606.x
12. Velázquez Pérez L, Cruz GS, Santos Falcón N, et al. (2009) Molecular epidemiology of spinocerebellar ataxias in Cuba: insights into SCA2 founder effect in Holguin. Neurosci Lett 454:157–60. doi: 10.1016/j.neulet.2009.03.015
13. Magaña JJ, Velázquez-Pérez L, Cisneros B (2013) Spinocerebellar ataxia type 2: clinical presentation, molecular mechanisms, and therapeutic perspectives. Mol Neurobiol 47:90–104. doi: 10.1007/s12035-012-8348-8
14. Schöls L, Bauer P, Schmidt T, et al. (2004) Autosomal dominant cerebellar ataxias: clinical features, genetics, and pathogenesis. Lancet Neurol 3:291–304. doi: 10.1016/S1474-4422(04)00737-9
15. Wadia NH, Swami RK (1971) A new form of heredo-familial spinocerebellar degeneration with slow eye movements (nine families). Brain 94:359–374. doi:

10.1093/brain/94.2.359

16. Sinha KK (2004) Autosomal dominant cerebellar ataxia: SCA2 is the most frequent mutation in eastern India. J Neurol Neurosur Ps 75:448–452. doi: 10.1136/jnnp.2002.004895
17. Pulst SM, Nechiporuk A, Nechiporuk T, et al. (1996) Moderate expansion of a normally biallelic trinucleotide repeat in spinocerebellar ataxia type 2. Nat Genet 14:269–76. doi: 10.1038/ng1196-269
18. Imbert G, Saudou F, Yvert G, et al. (1996) Cloning of the gene for spinocerebellar ataxia 2 reveals a locus with high sensitivity to expanded CAG/glutamine repeats. Nat Genet 14:285–91. doi: 10.1038/ng1196-285
19. Sanpei K, Takano H, Igarashi S, et al. (1996) Identification of the spinocerebellar ataxia type 2 gene using a direct identification of repeat expansion and cloning technique, DIRECT. Nat Genet 14:277–84. doi: 10.1038/ng1196-277
20. Velázquez-Pérez L, Rodríguez-Labrada R, García-Rodríguez JC, et al. (2011) A comprehensive review of spinocerebellar ataxia type 2 in Cuba. Cerebellum 10:184–98. doi: 10.1007/s12311-011-0265-2
21. Alonso E, Martínez-Ruano L, De Biase I, et al. (2007) Distinct distribution of autosomal dominant spinocerebellar ataxia in the Mexican population. Movement Disord 22:1050–3. doi: 10.1002/mds.21470
22. Leggo J, Dalton A, Morrison PJ, et al. (1997) Analysis of spinocerebellar ataxia types 1, 2, 3, and 6, dentatorubral-pallidoluysian atrophy, and Friedreich's ataxia genes in spinocerebellar ataxia patients in the UK. J Med Genet 34:982–5. doi: 10.1136/jmg.34.12.982
23. Giunti P, Sabbadini G, Sweeney MG, et al. (1998) The role of the SCA2 trinucleotide repeat expansion in 89 autosomal dominant cerebellar ataxia families. Frequency, clinical and genetic correlates. Brain 121 Pt 3:459–67. doi: 10.1093/brain/121.3.459
24. Infante J, Combarros O, Volpini V, et al. (2005) Autosomal dominant cerebellar ataxias in Spain: molecular and clinical correlations, prevalence estimation and survival analysis. Acta Neurol Scand 111:391–9. doi: 10.1111/j.1600-0404.2005.00400.x
25. Pujana MA, Corral J, Gratacòs M, et al. (1999) Spinocerebellar ataxias in Spanish patients: genetic analysis of familial and sporadic cases. The Ataxia Study Group. Hum Genet 104:516–22. doi: 10.1007/s004399900163
26. Lastres-Becker I, Rüb U, Auburger G (2008) Spinocerebellar ataxia 2 (SCA2). Cerebellum 7:115–24. doi: 10.1007/s12311-008-0019-y
27. Pagon RA, Adam MP, Ardinger HH, et al. (2015) GeneReviews®.
28. Bürk K, Abele M, Fetter M, et al. (1996) Autosomal dominant cerebellar ataxia type I clinical features and MRI in families with SCA1, SCA2 and SCA3. Brain 119 Pt 5:1497–505. doi: 10.1093/brain/119.5.1497
29. Klockgether T, Lüdtke R, Kramer B, et al. (1998) The natural history of degenerative ataxia: a retrospective study in 466 patients. Brain 121 Pt 4:589–600. doi: 10.1093/brain/121.4.589
30. Bürk K, Globas C, Bösch S, et al. (2003) Cognitive deficits in spinocerebellar ataxia type 1, 2, and 3. J Neurol 250:207–11. doi: 10.1007/s00415-003-0976-5

31. Lo RY, Figueroa KP, Pulst SM, et al. (2016) Depression and clinical progression in spinocerebellar ataxias. Parkinsonism Relat D 22:87–92. doi: 10.1016/j.parkreldis.2015.11.021

32. Estrada R, Galarraga J, Orozco G, et al. (1999) Spinocerebellar ataxia 2 (SCA2): morphometric analyses in 11 autopsies. Acta Neuropathol 97:306–310. doi: 10.1007/s004010050989

33. Pang JT, Giunti P, Chamberlain S, et al. (2002) Neuronal intranuclear inclusions in SCA2: a genetic, morphological and immunohistochemical study of two cases. Brain 125:656–63. doi: 10.1093/brain/awf060

34. Ishida C, Komai K, Yonezawa K, et al. (2011) An autopsy case of an aged patient with spinocerebellar ataxia type 2. Neuropathology 31:510–8. doi: 10.1111/j.1440-1789.2010.01176.x

35. Seidel K, Siswanto S, Brunt ERP, et al. (2012) Brain pathology of spinocerebellar ataxias. Acta Neuropathol 124:1–21. doi: 10.1007/s00401-012-1000-x

36. Rüb U, Schöls L, Paulson H, et al. (2013) Clinical features, neurogenetics and neuropathology of the polyglutamine spinocerebellar ataxias type 1, 2, 3, 6 and 7. Prog Neurobiol 104:38–66. doi: 10.1016/j.pneurobio.2013.01.001

37. Park H, Kim H-J, Jeon BS (2015) Parkinsonism in spinocerebellar ataxia. Biomed Res Int 2015:125273. doi: 10.1155/2015/125273

38. Koyano S, Uchihara T, Fujigasaki H, et al. (1999) Neuronal intranuclear inclusions in spinocerebellar ataxia type 2: triple-labeling immunofluorescent study. Neurosci Lett 273:117–20. doi: 10.1016/S0304-3940(99)00656-4

39. Sahba S, Nechiporuk A, Figueroa KP, et al. (1998) Genomic structure of the human gene for spinocerebellar ataxia type 2 (SCA2) on chromosome 12q24.1. Genomics 47:359–64. doi: 10.1006/geno.1997.5131

40. Shibata H, Huynh DP, Pulst SM (2000) A novel protein with RNA-binding motifs interacts with ataxin-2. Hum Mol Genet 9:1303–13.

41. Ng H, Pulst S-M, Huynh DP (2007) Ataxin-2 mediated cell death is dependent on domains downstream of the polyQ repeat. Exp Neurol 208:207–215. doi: 10.1016/j.expneurol.2007.07.023

42. Kiehl TR, Shibata H, Pulst SM (2000) The ortholog of human ataxin-2 is essential for early embryonic patterning in C. elegans. J Mol Neurosci 15:231–41. doi: 10.1385/JMN:15:3:231

43. Ciosk R, DePalma M, Priess JR (2004) ATX-2, the C. elegans ortholog of ataxin 2, functions in translational regulation in the germline. Development 131:4831–41. doi: 10.1242/dev.01352

44. Mangus DA, Amrani N, Jacobson A (1998) Pbp1p, a factor interacting with Saccharomyces cerevisiae poly(A)-binding protein, regulates polyadenylation. Mol Cell Biol 18:7383–96. doi: 10.1128/MCB.18.12.7383

45. Zhang Y, Ling J, Yuan C, et al. (2013) A role for Drosophila ATX2 in activation of PER translation and circadian behavior. Science 340:879–82. doi: 10.1126/science.1234746

46. Ralser M, Albrecht M, Nonhoff U, et al. (2005) An integrative approach to gain insights into the cellular function of human ataxin-2. J Mol Biol 346:203–14. doi: 10.1016/j.jmb.2004.11.024

47. Kiehl T-R, Nechiporuk A, Figueroa KP, et al. (2006) Generation and characterization of Sca2 (ataxin-2) knockout mice. Biochem Bioph Res Co 339:17–24. doi: 10.1016/j.bbrc.2005.10.186

48. Huynh DP, Maalouf M, Silva AJ, et al. (2009) Dissociated fear and spatial learning in mice with deficiency of ataxin-2. PLoS One 4:e6235. doi: 10.1371/journal.pone.0006235

49. Lastres-Becker I, Brodesser S, Lütjohann D, et al. (2008) Insulin receptor and lipid metabolism pathology in ataxin-2 knock-out mice. Hum Mol Genet 17:1465–81. doi: 10.1093/hmg/ddn035

50. Fittschen M, Lastres-Becker I, Halbach M V, et al. (2015) Genetic ablation of ataxin-2 increases several global translation factors in their transcript abundance but decreases translation rate. Neurogenetics 16:181–92. doi: 10.1007/s10048-015-0441-5

51. Chen Y, Huang R, Yang Y, et al. (2011) Ataxin-2 intermediate-length polyglutamine: a possible risk factor for Chinese patients with amyotrophic lateral sclerosis. Neurobiol Aging 32:1925.e1–5. doi: 10.1016/j.neurobiolaging.2011.05.015

52. Elden AC, Kim H-J, Hart MP, et al. (2010) Ataxin-2 intermediate-length polyglutamine expansions are associated with increased risk for ALS. Nature 466:1069–1075. doi: 10.1038/nature09320

53. Lee T, Li YR, Ingre C, et al. (2011) Ataxin-2 intermediate-length polyglutamine expansions in European ALS patients. Hum Mol Genet 20:1697–700. doi: 10.1093/hmg/ddr045

54. Al-Ramahi I, Pérez AM, Lim J, et al. (2007) dAtaxin-2 mediates expanded Ataxin-1-induced neurodegeneration in a Drosophila model of SCA1. PLoS Genet 3:e234. doi: 10.1371/journal.pgen.0030234

55. Uchihara T, Fujigasaki H, Koyano S, et al. (2001) Non-expanded polyglutamine proteins in intranuclear inclusions of hereditary ataxias--triple-labeling immunofluorescence study. Acta Neuropathol 102:149–52. doi: 10.1007/s004010100364

56. Lessing D, Bonini NM (2008) Polyglutamine genes interact to modulate the severity and progression of neurodegeneration in Drosophila. PLoS Biol 6:e29. doi: 10.1371/journal.pbio.0060029

57. Nóbrega C, Carmo-Silva S, Albuquerque D, et al. (2015) Re-establishing ataxin-2 downregulates translation of mutant ataxin-3 and alleviates Machado-Joseph disease. Brain 138:3537–54. doi: 10.1093/brain/awv298

58. von Campenhausen S, Winter Y, Rodrigues e Silva A, et al. (2011) Costs of illness and care in Parkinson's disease: an evaluation in six countries. Eur Neuropsychopharmacol 21:180–91. doi: 10.1016/j.euroneuro.2010.08.002

59. Brown RC, Lockwood AH, Sonawane BR (2005) Neurodegenerative diseases: an overview of environmental risk factors. Environ Health Perspect 113:1250–6.

60. Huynh DP, Figueroa K, Hoang N, Pulst SM (2000) Nuclear localization or inclusion body formation of ataxin-2 are not necessary for SCA2 pathogenesis in mouse or human. Nat Genet 26:44–50. doi: 10.1038/79162

61. Aguiar J, Fernández J, Aguilar A, et al. (2006) Ubiquitous expression of human

SCA2 gene under the regulation of the SCA2 self promoter cause specific Purkinje cell degeneration in transgenic mice. Neurosci Lett 392:202–6. doi: 10.1016/j.neulet.2005.09.020

62. Damrath E, Heck M V, Gispert S, et al. (2012) ATXN2-CAG42 sequesters PABPC1 into insolubility and induces FBXW8 in cerebellum of old ataxic knock-in mice. PLoS Genet 8:e1002920. doi: 10.1371/journal.pgen.1002920

63. Hansen ST, Meera P, Otis TS, Pulst SM (2013) Changes in Purkinje cell firing and gene expression precede behavioral pathology in a mouse model of SCA2. Hum Mol Genet 22:271–83. doi: 10.1093/hmg/dds427

64. Dansithong W, Paul S, Figueroa KP, et al. (2015) Ataxin-2 regulates RGS8 translation in a new BAC-SCA2 transgenic mouse model. PLoS Genet 11:e1005182. doi: 10.1371/journal.pgen.1005182

65. Liu J, Tang T-S, Tu H, et al. (2009) Deranged calcium signaling and neurodegeneration in spinocerebellar ataxia type 2. J Neurosci 29:9148–62. doi: 10.1523/JNEUROSCI.0660-09.2009

66. Kasumu AW, Liang X, Egorova P, et al. (2012) Chronic suppression of inositol 1,4,5-triphosphate receptor-mediated calcium signaling in cerebellar purkinje cells alleviates pathological phenotype in spinocerebellar ataxia 2 mice. J Neurosci 32:12786–96. doi: 10.1523/JNEUROSCI.1643-12.2012

67. Chang Y-K, Chen M-H, Chiang Y-H, et al. (2011) Mesenchymal stem cell transplantation ameliorates motor function deterioration of spinocerebellar ataxia by rescuing cerebellar Purkinje cells. J Biomed Sci 18:54. doi: 10.1186/1423-0127-18-54

68. Kasumu AW, Hougaard C, Rode F, et al. (2012) Selective positive modulator of calcium-activated potassium channels exerts beneficial effects in a mouse model of spinocerebellar ataxia type 2. Chem Biol 19:1340–53. doi: 10.1016/j.chembiol.2012.07.013

69. Halbach MV, Gispert S, Stehning T, et al. (2016) Atxn2 Knockout and CAG42-Knock-in Cerebellum Shows Similarly Dysregulated Expression in Calcium Homeostasis Pathway. Cerebellum. doi: 10.1007/s12311-016-0762-4

70. Tang T-S, Tu H, Chan EYW, et al. (2003) Huntingtin and huntingtin-associated protein 1 influence neuronal calcium signaling mediated by inositol-(1,4,5) triphosphate receptor type 1. Neuron 39:227–39. doi: 10.1016/S0896-6273(03)00366-0

71. Chen X, Tang T-S, Tu H, et al. (2008) Deranged calcium signaling and neurodegeneration in spinocerebellar ataxia type 3. J Neurosci 28:12713–24. doi: 10.1523/JNEUROSCI.3909-08.2008

72. Crum BA, Josephs KA (2006) Varied electrophysiologic patterns in spinocerebellar ataxia type 2. Eur J Neurol 13:194–7. doi: 10.1111/j.1468-1331.2006.01166.x

73. Velázquez Pérez L, Sánchez Cruz G, Canales Ochoa N, et al. (2007) Electrophysiological features in patients and presymptomatic relatives with spinocerebellar ataxia type 2. J Neurol Sci 263:158–64. doi: 10.1016/j.jns.2007.07.013

74. Van Keuren ML, Gavrilina GB, Filipiak WE, et al. (2009) Generating transgenic

mice from bacterial artificial chromosomes: transgenesis efficiency, integration and expression outcomes. Transgenic Res 18:769–85. doi: 10.1007/s11248-009-9271-2

75. Heintz N (2001) BAC to the future: the use of bac transgenic mice for neuroscience research. Nat Rev Neurosci 2:861–70. doi: 10.1038/35104049

76. Li Y, Liu W, Oo TF, et al. (2009) Mutant LRRK2(R1441G) BAC transgenic mice recapitulate cardinal features of Parkinson's disease. Nat Neurosci 12:826–8. doi: 10.1038/nn.2349

77. Gray M, Shirasaki DI, Cepeda C, et al. (2008) Full-Length Human Mutant Huntingtin with a Stable Polyglutamine Repeat Can Elicit Progressive and Selective Neuropathogenesis in BACHD Mice. J Neurosci 28:6182–6195. doi: 10.1523/JNEUROSCI.0857-08.2008

78. Ralser M, Nonhoff U, Albrecht M, et al. (2005) Ataxin-2 and huntingtin interact with endophilin-A complexes to function in plastin-associated pathways. Hum Mol Genet 14:2893–909. doi: 10.1093/hmg/ddi321

79. Satterfield TF, Jackson SM, Pallanck LJ (2002) A Drosophila homolog of the polyglutamine disease gene SCA2 is a dosage-sensitive regulator of actin filament formation. Genetics 162:1687–702.

80. Xia G, Santostefano K, Hamazaki T, et al. (2013) Generation of human-induced pluripotent stem cells to model spinocerebellar ataxia type 2 in vitro. J Mol Neurosci 51:237–48. doi: 10.1007/s12031-012-9930-2

81. Déglon N, Tseng JL, Bensadoun JC, et al. (2000) Self-inactivating lentiviral vectors with enhanced transgene expression as potential gene transfer system in Parkinson's disease. Hum Gene Ther 11:179–90. doi: 10.1089/10430340050016256

82. de Almeida LP, Ross CA, Zala D, et al. (2002) Lentiviral-Mediated Delivery of Mutant Huntingtin in the Striatum of Rats Induces a Selective Neuropathology Modulated by Polyglutamine Repeat Size, Huntingtin Expression Levels, and Protein Length. J Neurosci 22:3473–3483.

83. Carpenter AE, Jones TR, Lamprecht MR, et al. (2006) CellProfiler: image analysis software for identifying and quantifying cell phenotypes. Genome Biol 7:R100. doi: 10.1186/gb-2006-7-10-r100

84. Gornicka-Pawlak E, Janowski M, Jablonska A, et al. (2015) Complex assessment of distinct cognitive impairments following ouabain injection into the rat dorsoloateral striatum. Behav Brain Res 289:133–140. doi: 10.1016/j.bbr.2015.03.061

85. Vandesompele J, De Preter K, Pattyn F, et al. (2002) Accurate normalization of real-time quantitative RT-PCR data by geometric averaging of multiple internal control genes. Genome Biol 3:RESEARCH0034.

86. Andersen CL, Jensen JL, Ørntoft TF (2004) Normalization of real-time quantitative reverse transcription-PCR data: a model-based variance estimation approach to identify genes suited for normalization, applied to bladder and colon cancer data sets. Cancer Res 64:5245–50. doi: 10.1158/0008-5472.CAN-04-0496

87. de Almeida LP, Zala D, Aebischer P, Déglon N (2001) Neuroprotective Effect of a CNTF-Expressing Lentiviral Vector in the Quinolinic Acid Rat Model of

Huntington's Disease. Neurobiol Dis 8:433–446. doi: 10.1006/nbdi.2001.0388

88. Zala D, Bensadoun J-C, Pereira de Almeida L, et al. (2004) Long-term lentiviral-mediated expression of ciliary neurotrophic factor in the striatum of Huntington's disease transgenic mice. Exp Neurol 185:26–35. doi: 10.1016/j.expneurol.2003.09.002
89. Nóbrega C, Nascimento-Ferreira I, Onofre I, et al. (2013) Overexpression of mutant ataxin-3 in mouse cerebellum induces ataxia and cerebellar neuropathology. Cerebellum 12:441–55. doi: 10.1007/s12311-012-0432-0
90. Lauwers E, Debyser Z, Dorpe J, et al. (2006) Neuropathology and Neurodegeneration in Rodent Brain Induced by Lentiviral Vectormediated Overexpression of α-Synuclein. Brain Pathol 13:364–372. doi: 10.1111/j.1750-3639.2003.tb00035.x
91. Alves S, Régulier E, Nascimento-Ferreira I, et al. (2008) Striatal and nigral pathology in a lentiviral rat model of Machado-Joseph disease. Hum Mol Genet 17:2071–83. doi: 10.1093/hmg/ddn106
92. Lamprecht MR, Sabatini DM, Carpenter AE (2007) CellProfiler™: free, versatile software for automated biological image analysis. Biotechniques 42:71–75.
93. Feng Q, Ma Y, Mu S, et al. (2014) Specific reactions of different striatal neuron types in morphology induced by quinolinic acid in rats. PLoS One 9:e91512. doi: 10.1371/journal.pone.0091512
94. Schneider CA, Rasband WS, Eliceiri KW (2012) NIH Image to ImageJ: 25 years of image analysis. Nat Methods 9:671–675. doi: 10.1038/nmeth.2089
95. Hong H, Kim BS, Im H-I (2016) Pathophysiological Role of Neuroinflammation in Neurodegenerative Diseases and Psychiatric Disorders. Int Neurourol J 20:S2–7. doi: 10.5213/inj.1632604.302
96. Yin HH, Knowlton BJ (2006) The role of the basal ganglia in habit formation. Nat Rev Neurosci 7:464–476. doi: 10.1038/nrn1919
97. Cooper-Knock J, Kirby J, Ferraiuolo L, et al. (2012) Gene expression profiling in human neurodegenerative disease. Nat Rev Neurol 8:518–530. doi: 10.1038/nrneurol.2012.156
98. Khaminets A, Behl C, Dikic I (2016) Ubiquitin-Dependent And Independent Signals In Selective Autophagy. Trends Cell Biol 26:6–16. doi: 10.1016/j.tcb.2015.08.010
99. Goker-Alpan O, Stubblefield BK, Giasson BI, Sidransky E (2010) Glucocerebrosidase is present in α-synuclein inclusions in Lewy body disorders. Acta Neuropathol 120:641–9. doi: 10.1007/s00401-010-0741-7
100. Gómez-Tortosa E, Newell K, Irizarry MC, et al. (2000) α-Synuclein immunoreactivity in dementia with Lewy bodies: morphological staging and comparison with ubiquitin immunostaining. Acta Neuropathol 99:352–357. doi: 10.1007/s004010051135
101. Shults CW (2006) Lewy bodies. Proc Natl Acad Sci U S A 103:1661–8. doi: 10.1073/pnas.0509567103
102. Scheggi S, Rauggi R, Gambarana C, et al. (2004) Dopamine and cyclic AMP-regulated phosphoprotein-32 phosphorylation pattern in cocaine and morphine-sensitized rats. J Neurochem 90:792–799. doi: 10.1111/j.1471-4159.2004.02510.x

103. Ouimet CC, Miller PE, Hemmings HC, et al. (1984) DARPP-32, a dopamine- and adenosine 3’:5'-monophosphate-regulated phosphoprotein enriched in dopamine-innervated brain regions. III. Immunocytochemical localization. J Neurosci 4:111–24.

104. Ben Haim L, Carrillo-de Sauvage M-A, Ceyzériat K, Escartin C (2015) Elusive roles for reactive astrocytes in neurodegenerative diseases. Front Cell Neurosci 9:278. doi: 10.3389/fncel.2015.00278

105. Maragakis NJ, Rothstein JD (2006) Mechanisms of Disease: astrocytes in neurodegenerative disease. Nat Clin Pract Neurol 2:679–689. doi: 10.1038/ncpneuro0355

106. Roy A, Fung YK, Liu X, Pahan K (2006) Up-regulation of microglial CD11b expression by nitric oxide. J Biol Chem 281:14971–80. doi: 10.1074/jbc.M600236200

107. Ito D, Tanaka K, Suzuki S, et al. (2001) Enhanced expression of Iba1, ionized calcium-binding adapter molecule 1, after transient focal cerebral ischemia in rat brain. Stroke 32:1208–15.

108. Huynh DP, Del Bigio MR, Ho DH, Pulst SM (1999) Expression of ataxin-2 in brains from normal individuals and patients with Alzheimer’s disease and spinocerebellar ataxia 2. Ann Neurol 45:232–41.

109. Kwon SE, Chapman ER (2011) Synaptophysin regulates the kinetics of synaptic vesicle endocytosis in central neurons. Neuron 70:847–54. doi: 10.1016/j.neuron.2011.04.001

110. Eshkind LG, Leube RE (1995) Mice lacking synaptophysin reproduce and form typical synaptic vesicles. Cell Tissue Res 282:423–33.

111. McMahon HT, Bolshakov VY, Janz R, et al. (1996) Synaptophysin, a major synaptic vesicle protein, is not essential for neurotransmitter release. Proc Natl Acad Sci U S A 93:4760–4.

112. Janz R, Südhof TC, Hammer RE, et al. (1999) Essential Roles in Synaptic Plasticity for Synaptogyrin I and Synaptophysin I. Neuron 24:687–700. doi: 10.1016/S0896-6273(00)81122-8

113. Schmitt U, Tanimoto N, Seeliger M, et al. (2009) Detection of behavioral alterations and learning deficits in mice lacking synaptophysin. Neuroscience 162:234–243. doi: 10.1016/j.neuroscience.2009.04.046

114. van de Loo S, Eich F, Nonis D, et al. (2009) Ataxin-2 associates with rough endoplasmic reticulum. Exp Neurol 215:110–118. doi: 10.1016/j.expneurol.2008.09.020

115. Tarun SZ, Sachs AB (1996) Association of the yeast poly(A) tail binding protein with translation initiation factor eIF-4G. EMBO J 15:7168–77.

116. Pedroso JL, Braga-Neto P, Escorcio-Bezerra ML, et al. (2016) Non-motor and Extracerebellar Features in Spinocerebellar Ataxia Type 2. Cerebellum. doi: 10.1007/s12311-016-0761-5

117. Abdel-Aleem A, Zaki MS (2008) Spinocerebellar ataxia type 2 (SCA2) in an Egyptian family presenting with polyphagia and marked CAG expansion in infancy. J Neurol 255:413–9. doi: 10.1007/s00415-008-0690-4

118. Kiehl T-R, Nechiporuk A, Figueroa KP, et al. (2006) Generation and

characterization of Sca2 (ataxin-2) knockout mice. Biochem Bioph Res Co 339:17–24. doi: 10.1016/j.bbrc.2005.10.186

119. Brüning JC, Gautam D, Burks DJ, et al. (2000) Role of brain insulin receptor in control of body weight and reproduction. Science 289:2122–5.
120. Pycock CJ (1980) Turning behaviour in animals. Neuroscience 5:461–514. doi: 10.1016/0306-4522(80)90048-2
121. Schwarting RKW, Huston JP (1996) The unilateral 6-hydroxydopamine lesion model in behavioral brain research. Analysis of functional deficits, recovery and treatments. Prog Neurobiol 50:275–331. doi: 10.1016/S0301-0082(96)00040-8
122. Furtado S, Payami H, Lockhart PJ, et al. (2004) Profile of families with parkinsonism-predominant spinocerebellar ataxia type 2 (SCA2). Mov Disord 19:622–629. doi: 10.1002/mds.20074
123. Lu C-S, Wu Chou Y-H, Yen T-C, et al. (2002) Dopa-responsive parkinsonism phenotype of spinocerebellar ataxia type 2. Movement Disord 17:1046–51. doi: 10.1002/mds.10243
124. Varrone A, Salvatore E, De Michele G, et al. (2004) Reduced striatal [123 I]FP-CIT binding in SCA2 patients without parkinsonism. Ann Neurol 55:426–30. doi: 10.1002/ana.20054
125. Reimold M, Globas C, Gleichmann M, et al. (2006) Spinocerebellar ataxia type 1, 2, and 3 and restless legs syndrome: striatal dopamine D2 receptor status investigated by [11C]raclopride positron emission tomography. Movement Disord 21:1667–73. doi: 10.1002/mds.20978

Chapter VII – Supplementary material

Supplementary figure S1

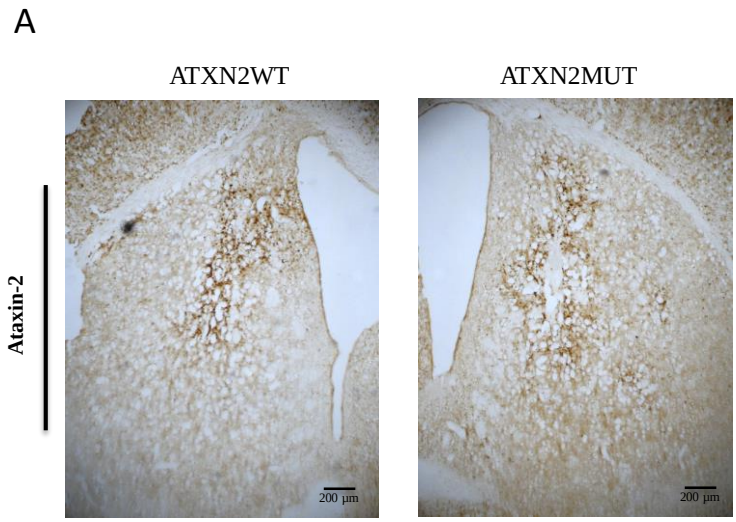

Figure S1. Ataxin-2 wide expression in the *striatum*. (A) This representative picture shows the robust and wide expression of both WT and mutant ataxin-2 throughout the *striatum*.

Supplementary figure S2

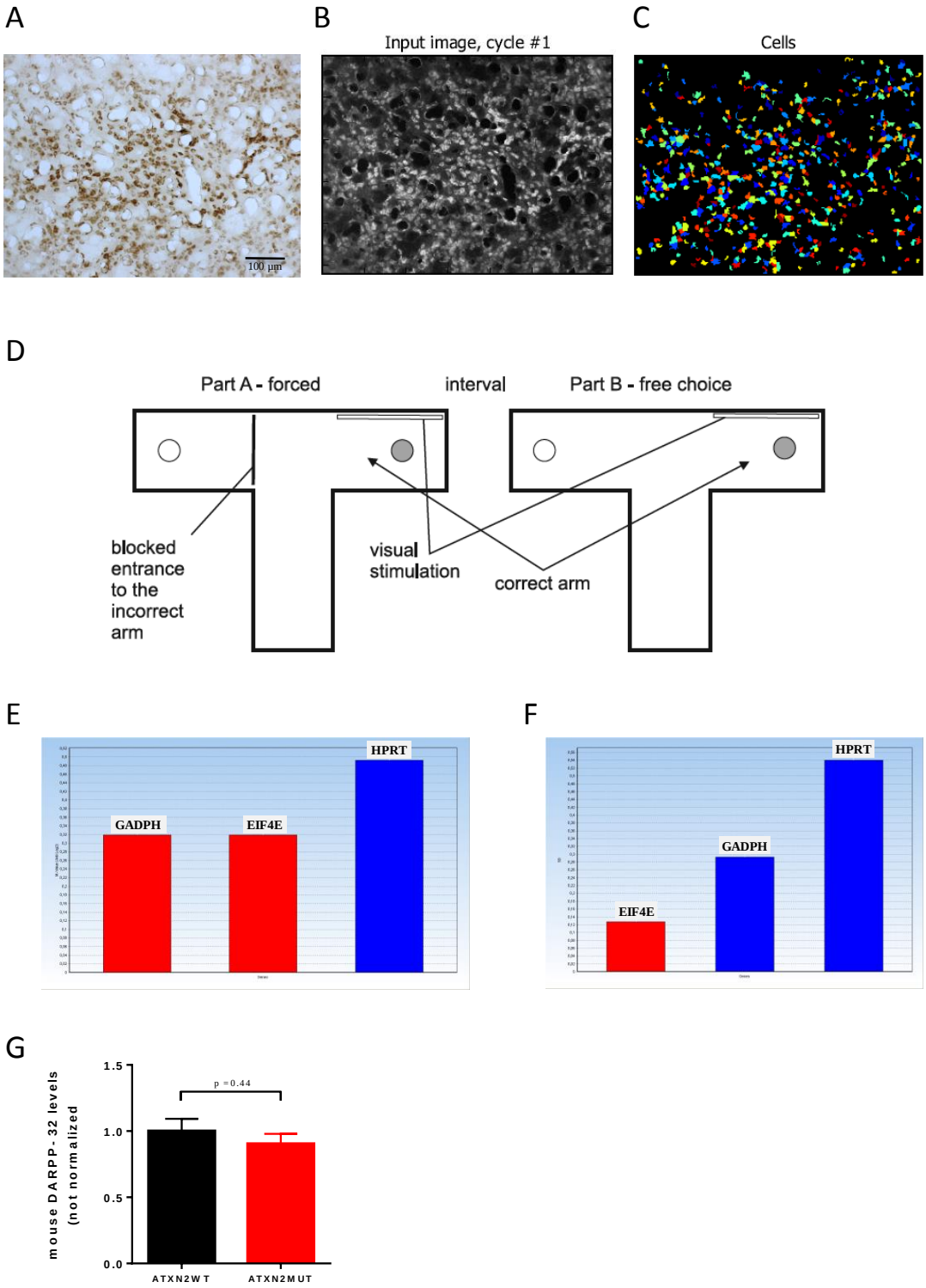

Figure S2. Representative figures and examples of several experimental procedures. (A) An original image of a section stained with antibodies anti-ataxin-2 **(B and C)** and the output of CellProfiler after the

analysis of that image. The software starts by converting the figure into a black and white format and then into a system of colors, representing the intensity displayed by each transduced cell. **(D)** Schematic representation of the "learning day" of the T-maze test. In the forced step, one arm of the arena is obstructed and the mice is therefore compelled to enter the only accessible side, which has a food reward and a visual cue (white rectangle attached to the wall). The free choice part is equal to the forced part with the exception that both arms of the maze are available. This image was retrieved from [84] **(E)** Representative output files of the geNorm and **(F)** NormFinder, both calculating HPRT as the least constant gene among different conditions. **(G)** Non-normalized quantification of DARPP32 in western-blot analysis, showing stable values in both experimental conditions. Data is presented as mean ± SEM, unpaired student's t-test.

Supplementary figure S3

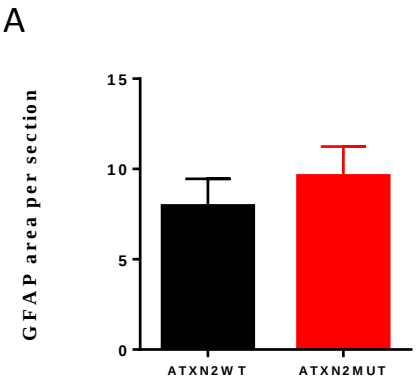

Figure S3. GFAP area per section. (A) There are no significant differences in the area of astrogliosis between the two hemispheres of the *striatum*. A total of 8 sections from 4 bilaterally injected mice were used (n=4) and quantified with ImageJ software. Data is presented as mean ± SEM. *p<0.05, paired student's t-test.

Supplementary figure S4

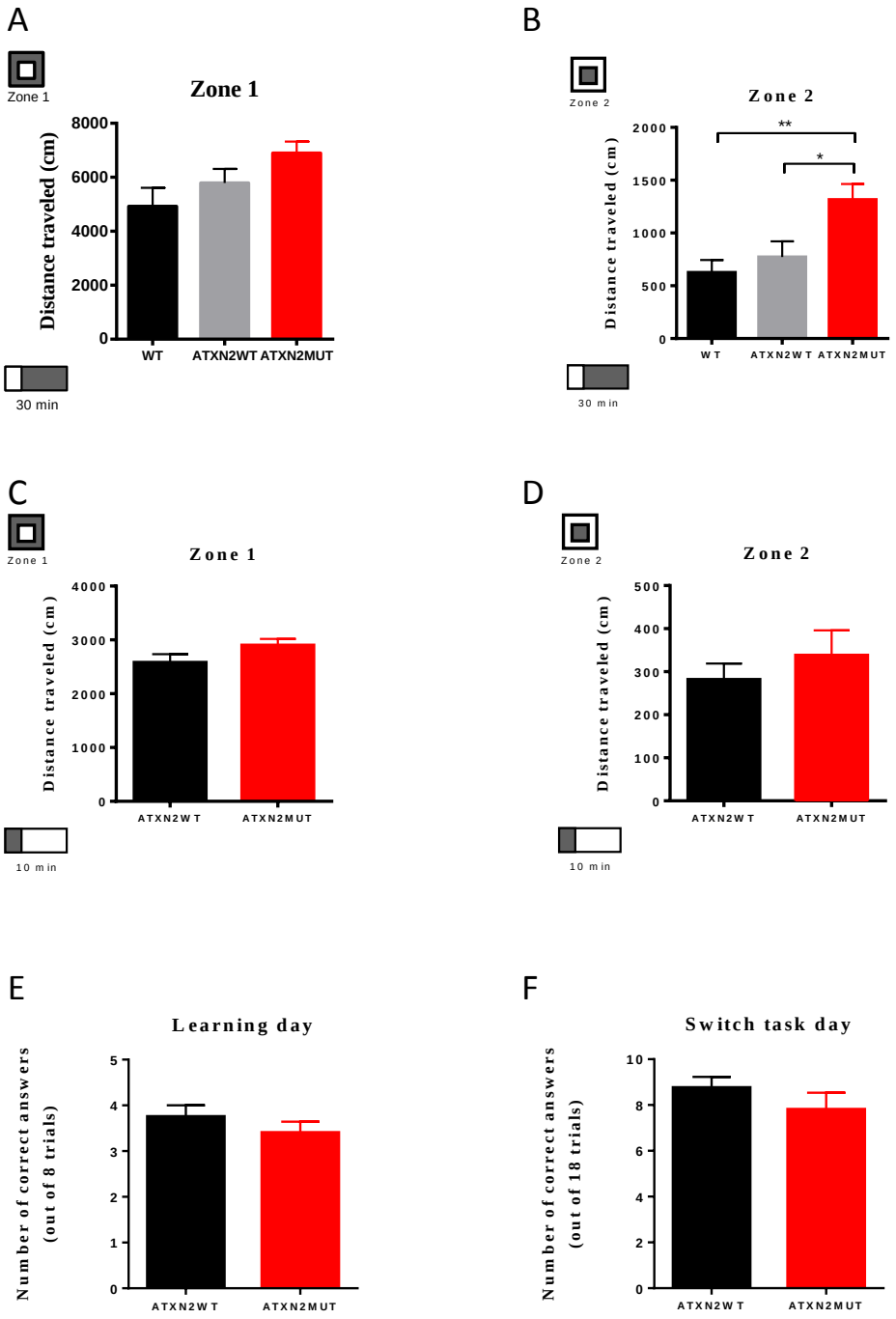

Figure S4. The animals injected with ATXN2MUT systematically covered longer distances than the control ones (injected with ATXN2WT) but showed no learning disabilities. **(A-D)** The animals overexpressing the mutant form of ataxin-2 (n=8) systematically tended to cover longer distances than both the control group (overexpressing the WT form of the protein) (n=9) and the WT littermates (n=5). This

tendency is present in all the time points and the two different zones measured and is sometimes significant. **(E and F)** There were no differences in cognitive behavior between the mice injected with ATXN2MUT (n=5) and the ones injected with ATXN2WT (n=4). Data is presented as mean ± SEM. *$p<0.05$, paired student's t-test.